On single-tap equalization for an FBMC multicarrier system in wireless channels

Davide Mattera, Mario Tanda, Maurice Bellanger

On single-tap equalization for FBMC multicarrier systems in wireless channels

Davide Mattera[a], Mario Tanda[a,*], Maurice Bellanger[b]

[a]*Dipartimento di Ingegneria Elettrica e delle Tecnologie dell'Informazione, Università degli Studi di Napoli Federico II, via Claudio 21, I-80125 Napoli, Italy.*
[b]*CNAM-Electronique, 292 rue Saint-Martin, 75141 Paris cedex 03, France.*

Abstract

This paper deals with single-tap equalization for the recently introduced FBMC-PAM system, a multicarrier scheme able to meet the requirements of cognitive radio such as high level of adjacent channel leakage ratio and asynchronous communications. The optimum single-tap gain in the minimum mean square error (MMSE) sense is derived and its performance is compared with that of previously considered receivers. It is shown that when the optimum MMSE single-tap gain is multiplied (before the real part extraction) by a zero-mean complex noncircular random variable (that is, when the zero-mean output of the standard matched filter has a complementary variance different from zero) the achieved performance can be better than that of other single-tap receivers and similar to that of a more advanced previously considered equalization structure.

Keywords: FBMC, single-tap equalization, MMSE, PAM, dispersive channel

*Corresponding author. Tel. +39-081-768-3791. Fax +39-081-768-5925.
Email addresses: mattera@unina.it (Davide Mattera), tanda@unina.it (Mario Tanda), bellang@cnam.fr (Maurice Bellanger)

1. Introduction

Filter bank multicarrier (FBMC) techniques are potential alternatives to the current orthogonal frequency division multiplexing (OFDM) schemes for some emerging applications fields such as machine type communications or cognitive radio [1]. In these systems the prototype filter controls performance and a number of operational aspects. Long filters assure high of out-of-band attenuation and asynchronous user coexistence. However, for reduced system latency short prototype filters are required.

In [2, 3] short prototype filters with overlapping factor K= 2 (i.e., only 2 adjacent multicarrier symbols overlap in time), have been proposed. Since FBMC offset-quadrature amplitude modulation (OQAM) combined with short filters assures limited performance, the complex lapped transform has been used for the design of the FBMC-PAM transceiver [4–6]. For a special choice of the prototype filter it is much similar to the first analog multicarrier system introduced by Chang [7]. The scheme is based on pulse amplitude modulation (PAM) combined with a sine prototype filter with overlapping factor K=2 and it achieves perfect reconstruction in the real field. Moreover, the sine prototype filter has a main lobe in the frequency domain whose width is 3 times the sub-carrier spacing while it is only 2 times for OFDM scheme. For this reason and for its better spectral decay, FBMC-PAM outperforms OFDM systems as well as FBMC-OQAM systems in terms of CFO sensitivity [8].

Several equalization structures have been considered for FBMC-PAM systems, among them the well known single-tap zero-forcing equalizer and the more advanced structures termed 2M-4M and 2M-6M [4]. In particular, the 2M-4M receiver evaluates the FFT of the received signal in a window of length 4M whose central part of length 2M is used by the single-tap receivers, divide this FFT by that of the channel in a window of the same length, performs the inverse FFT of

the resulting data and, then, uses the central part of length 2M as the input of the receiver for the AWGN channel.

This paper deals with single-tap equalization of FBMC-PAM signals in wireless dispersive channels. The optimum single-tap gain in the minimum mean square error (MMSE) sense is derived and it is shown that it assumes a more involved expression when the output of the standard matched filter (that multiplied by the considered gain and after real part extraction provides the decision variable) is noncircular [9–12], that is when its complementary variance is different from zero. Moreover, it is shown through computer simulations, that in this case the optimum MMSE single-tap equalizer can outperform other well-known single-tap structures and can assure a performance similar to that of the more advanced 2M-4M receiver.

The organization of the paper is as follows. In Section 2, the standard FBMC-PAM system is recalled. In Section 3 the MMSE single-tap gain expression is derived while in Section 4 and in Section 5, the single-path case and the asymptotic case (large number of subcarriers), respectively, are analyzed. Simulation results are reported in Section 6 and conclusions are drawn in the final Section.

It is shown that when the optimum MMSE single-tap gain is multiplied (before the real part extraction) by a zero-mean complex noncircular random variable (that is, when the zero-mean output of the standard matched filter has a complementary variance different from zero) the achieved performance can be better than that of other single-tap receivers and similar to that of a more advanced previously considered equalization structure.

Notation: $j \triangleq \sqrt{-1}$, superscript $(\cdot)^*$ denotes the complex conjugation, $\Re[\cdot]$ the real part, $\Im[\cdot]$ the imaginary part, $\delta[k]$ the Kronecker delta, $|\cdot|$ the absolute value, $\angle[\cdot]$ the argument of a complex number in $[-\pi, \pi)$ and $E[\cdot]$ denotes statistical expectation.

2. System Model

Let us consider an FBMC-PAM system [4] with $2M$ subcarriers. The received signal in time-dispersive channel can be written as

$$r(t) = \sum_{p=0}^{L-1} g_p \, s(t - \tau_p) + n(t) \tag{1}$$

where $s(t)$ is the transmitted FBMC-PAM signal, $n(t)$ denotes the zero-mean circular complex white Gaussian noise with independent real and imaginary parts, each with two sided power spectral density N_o, and τ_p is the delay of the pth path with complex gain g_p. The FBMC-PAM signal $s(t)$ is equal to

$$s(t) = \sum_{i=0}^{N_s-1} \sum_{k=0}^{2M-1} d_k[i] \, e^{j\frac{\pi}{T}\left(k+\frac{1}{2}\right)\left(t-iT+\frac{T}{2}\right)} \, h(t - iT) \tag{2}$$

where $2T$ is the FBMC-PAM symbol duration, N_s is the number of payload symbols, $d_k[i]$ is the real information symbol transmitted on the kth subcarrier in the ith symbol interval, and $h(t)$ is the real pulse-shaping filter. The data symbols are zero-mean statistically independent real random variables with mean-square value P_d, thus,

$$E\left\{d_k[i] d_m[l]\right\} = \delta[k - m] \, \delta[i - l] \, P_d. \tag{3}$$

In (1) the complex gains g_p are modeled as a zero-mean complex circular Gaussian random variables with variance σ_p^2 and statistically independent of one another. Moreover, it is assumed that the following condition holds

$$\sum_{p=0}^{L-1} \sigma_p^2 = 1. \tag{4}$$

The received signal $r(t)$ is filtered with an ideal low-pass filter with a bandwidth of $1/T_s$, where T_s denotes the sampling period (the FBMC-PAM symbol duration is equal to $2T = 2MT_s$), thus the discrete-time low-pass version of the received

signal can be written as

$$r[l] = \sum_{i=0}^{N_s-1} \sum_{k=0}^{2M-1} \sum_{p=0}^{L-1} g_p \, d_k[i] \, T_c[k, l - \theta_p - iM] + v[l] \tag{5}$$

where

$$T_c[k, l] \triangleq h[l] \, e^{j\frac{\pi}{M}\left(k+\frac{1}{2}\right)\left(l+\frac{1}{2}+\frac{M}{2}\right)}, \tag{6}$$

$\theta_p = \tau_p/T_s$ is the normalized delay of the pth path and $v[l]$ is a discrete-time zero-mean AWGN process with autocorrelation function

$$R_v[m] = E\left\{v[l]v^*[l-m]\right\} = \frac{2N_o}{T_s}\,\delta[m] = \sigma_v^2\,\delta[m]. \tag{7}$$

It is assumed that the normalized delays $\theta_p = \tau_p/T_s$ in (5) are integer values. In (6) the real prototype filter $h[l]$, equal to zero for $l \notin \mathcal{K}_{2M} \triangleq \{0, 1, \ldots, 2M-1\}$ and with energy

$$\mathcal{E}_h \triangleq \sum_{l=0}^{2M-1} h^2[l], \tag{8}$$

satisfies the following conditions

$$h[M + l] = h[M - l - 1] \qquad \forall\ l, \tag{9}$$

$$\sum_{m=-\infty}^{+\infty} h[l + mM]h[l + mM + 2rM] = \delta[r] \qquad \forall\ l, r \tag{10}$$

that imply the orthogonality condition in the real field

$$\Re\left\{\frac{1}{M}\sum_{l=0}^{2M-1} T_c[k, l]T_c^*[m, l - pM]\right\} = \delta[m - k]\,\delta[p]. \tag{11}$$

In this case, it follows that [4] in AWGN channel the optimum (in the maximum likelihood sense) decision variable for estimating statistically independent information symbols can be written as $\Re\left\{\hat{D}_m[i]\right\}$ where

$$\hat{D}_m[i] \triangleq \frac{1}{M}\sum_{l=0}^{2M-1} r[iM + l]T_c^*[m, l] \tag{12}$$

since conditions (9) and (10) assure the absence of intersymbol interference and intercarrier interference.

In the following it is considered the prototype filter

$$h[l] = \sin\left[\frac{\pi}{2M}\left(l+\frac{1}{2}\right)\right] \quad l \in \mathcal{K}_{2M}, \qquad h[l] = 0 \quad l \notin \mathcal{K}_{2M}. \tag{13}$$

This prototype filter satisfies conditions (9) and (10) and simplifies the receiver as shown in [4].

3. Optimum single-tap receiver

In this section we derive the optimum (in the minimum mean-square error (MMSE) sense) single-tap receiver for the signal model in (5). Specifically, we derive the expression of the complex gain a_m such that the estimate of the symbol transmitted on the $m-$th subcarrier in the $i-$th interval

$$\hat{d}_m[i] = \Re\left\{a_m \hat{D}_m[i]\right\} \tag{14}$$

minimizes the mean-square error

$$E\left[\epsilon^2\right] = E\left[\left(\hat{d}_m[i] - d_m[i]\right)^2\right]. \tag{15}$$

In (14) $\hat{D}_m[i]$ is the decision variable for AWGN (see (12)) evaluated by the receiver and a_m is the complex gain used by the single-tap equalizer to achieve satisfactory performance in a multipath channel. By substituting (14) in (15) and taking into account that

$$\Re^2\{\mathcal{A}\} = \frac{1}{2}\Re\left\{\mathcal{A}^2\right\} + \frac{1}{2} \mid \mathcal{A} \mid^2 \tag{16}$$

it follows that

$$E\left[\epsilon^2\right] = \frac{1}{2}\Re\left\{a_m^2 E\left[\hat{D}_m^2[i]\right]\right\} + \frac{1}{2} \mid a_m \mid^2 E\left[\left|\hat{D}_m[i]\right|^2\right] + P_d - 2\Re\left\{a_m E\left[d_m[i]\hat{D}_m[i]\right]\right\}. \tag{17}$$

A necessary and sufficient condition for a point a_m^o to be a stationary point for the real-valued function (17) analytic in both a_m and a_m^* is that the derivative is zero in a_m^o when a_m and a_m^* are considered as independent variables [13]. In particular, the real-valued function (17) can be minimized by solving the equation

$$a_m E\left[\hat{D}_m^2[i]\right] + a_m^* E\left[\left|\hat{D}_m[i]\right|^2\right] = 2E\left[d_m[i]\hat{D}_m[i]\right] . \tag{18}$$

In the derivation of (18) the following relationships

$$\frac{\partial}{\partial a_m}\Re\left\{a_m^2\,\gamma\right\} = \frac{\partial}{\partial a_m}\frac{1}{2}\left\{a_m^2\,\gamma + \left(a_m^2\right)^*\,\gamma^*\right\} = a_m\,\gamma \tag{19}$$

$$\frac{\partial}{\partial a_m}\Re\left\{a_m\,\gamma\right\} = \frac{\partial}{\partial a_m}\frac{1}{2}\left\{a_m\,\gamma + a_m^*\,\gamma^*\right\} = \frac{1}{2}\,\gamma \tag{20}$$

$$\frac{\partial}{\partial a_m}\gamma\;|\,a_m\,|^2 = \frac{\partial}{\partial a_m}\gamma\,a_m\,a_m^* = \gamma\,a_m^* \tag{21}$$

have been accounted for, where γ is any complex constant.

The solution of (18) (see Appendix A) leads to the following expression for the complex gain to be used in the optimum MMSE single-tap receiver

$$a_m^o = \frac{2E\left[d_m[i]\hat{D}_m[i]\right]E^*\left[\hat{D}_m^2[i]\right] - 2E^*\left[d_m[i]\hat{D}_m[i]\right]E\left[|\,\hat{D}_m[i]\,|^2\right]}{\left|E\left[\hat{D}_m^2[i]\right]\right|^2 - E^2\left[\left|\hat{D}_m[i]\right|^2\right]} . \tag{22}$$

It is worthwhile to emphasize that the optimum gain a_m^o depends not only on the terms $E\left[|\,\hat{D}_m[i]\,|^2\right]$ and $E\left[d_m[i]\hat{D}_m[i]\right]$ but also on the complementary variance $E\left[\hat{D}_m^2[i]\right]$ which is different from zero when the zero-mean complex random variable $\hat{D}_m[i]$ is noncircular [9–12]. Note that when $E\left[\hat{D}_m^2[i]\right] = 0$ the solution of (18) can be immediately obtained and is coincident with (22) in the particular case $E\left[\hat{D}_m^2[i]\right] = 0$.

By substituting (22) in (17) we obtain the expression of the minimum MSE value (see Appendix B)

$$E\left[\epsilon^2\right]_{\min} = P_d + 2\,\frac{\Re\left\{E^*\left[\hat{D}_m^2[i]\right]E^2\left[d_m[i]\hat{D}_m[i]\right]\right\} - E\left[\left|\hat{D}_m[i]\right|^2\right]\left|E\left[d_m[i]\hat{D}_m[i]\right]\right|^2}{E^2\left[\left|\hat{D}_m[i]\right|^2\right] - \left|E\left[\hat{D}_m^2[i]\right]\right|^2} . \tag{23}$$

In particular, if we define

$$\rho \stackrel{\triangle}{=} \frac{E\left[\hat{D}_m^2[i]\right]}{E\left[\left|\hat{D}_m[i]\right|^2\right]} \tag{24}$$

and

$$u \stackrel{\triangle}{=} \frac{E^2\left[d_m[i]\hat{D}_m[i]\right]}{E\left[\left|\hat{D}_m[i]\right|^2\right]} \tag{25}$$

we can write

$$E\left[\epsilon^2\right]_{\min} = P_d - \frac{2}{1-\mid \rho \mid^2}\left\{\mid u \mid -\Re\left[\rho^* u\right]\right\} . \tag{26}$$

Let us note that the second term in the right-hand side of (26) is positive since $\mid \rho \mid \leq 1$ and, then,

$$\Re\left[\rho^* u\right] \leq \mid \rho \mid \mid u \mid \leq \mid u \mid .$$

Taking into account (12) and (5) it follows that

$$\hat{D}_m[i] = \sum_{k=0}^{2M-1} \sum_q d_k(q)\, w_{m,k}(i-q) + N_m(i) \tag{27}$$

where

$$w_{m,k}(i-q) \stackrel{\triangle}{=} \frac{1}{M} \sum_{p=0}^{L-1} g_p \sum_{l=0}^{2M-1} T_c[k, l-\theta_p+(i-q)M]\, T_c^*[m,l] \tag{28}$$

and

$$N_m(i) \stackrel{\triangle}{=} \frac{1}{M} \sum_{l=0}^{2M-1} \nu[l+iM]\, T_c^*[m,l]. \tag{29}$$

In particular, the gain of the useful term in (27) is given by

$$g_u \stackrel{\triangle}{=} w_{m,m}(0) = \frac{1}{M} \sum_{p=0}^{L-1} g_p \sum_{l=0}^{2M-1} T_c[m, l-\theta_p]\, T_c^*[m,l] \tag{30}$$

Since the noise samples $\nu[l]$ are zero-mean complex circular statistically independent Gaussian random variables with variance σ_ν^2, it follows that

$$E\left[\hat{D}_m^2[i]\right] = P_d \sum_{k=0}^{2M-1} \sum_q w_{m,k}^2(i-q) \tag{31}$$

$$E\left[d_m[i]\hat{D}_m[i]\right] = P_d\, w_{m,m}(0) \tag{32}$$

and

$$E\left[\left|\hat{D}_m[i]\right|^2\right] = P_d\left(\sum_{k=0}^{2M-1}\sum_{q}\left|w_{m,k}(i-q)\right|^2 + \frac{1}{SNR}\right) \tag{33}$$

where

$$SNR \triangleq \frac{P_d\,\mathcal{E}_h}{\sigma_\nu^2}. \tag{34}$$

Thus, by using (31), (32) and (33) the optimum single-tap (22) can be obtained. Moreover, the corresponding minimum MSE value can be obtained by substituting in (26)

$$\rho = \frac{\displaystyle\sum_{k=0}^{2M-1}\sum_{q} w_{m,k}^2(i-q)}{\displaystyle\sum_{k=0}^{2M-1}\sum_{q}\left|w_{m,k}(i-q)\right|^2 + \frac{1}{SNR}} \tag{35}$$

and

$$u = \frac{P_d\, w_{m,m}^2(0)}{\displaystyle\sum_{k=0}^{2M-1}\sum_{q}\left|w_{m,k}(i-q)\right|^2 + \frac{1}{SNR}}\,. \tag{36}$$

4. The single-path case

Let us consider the case of a single-path channel, that is $L = 1$ in (5) and let us assume, without a loss of generality, that $\theta_o = 0$. It is shown in Appendix C that in this case

$$\sum_{k=0}^{2M-1}\sum_{q}\left(\frac{1}{M}\sum_{l=0}^{2M-1} T_c[k, l+(i-q)M]\, T_c^*[m,l]\right)^2 = 0 \tag{37}$$

while it is shown in Appendix D that

$$\sum_{k=0}^{2M-1}\sum_{q}\left|\frac{1}{M}\sum_{l=0}^{2M-1} T_c[k, l+(i-q)M]\, T_c^*[m,l]\right|^2 = 2\,, \tag{38}$$

therefore, accounting for (31), (28) and (37) we can write

$$E\left[\hat{D}_m^2[i]\right] = P_d\, g_0^2 \sum_{k=0}^{2M-1} \sum_{q} \left(\frac{1}{M} \sum_{l=0}^{2M-1} T_c[k, l+(i-q)M]\, T_c^*[m,l] \right)^2 = 0. \tag{39}$$

Moreover, from (32), (28) and (11) it results that

$$E\left[d_m[i]\hat{D}_m[i]\right] = P_d\, g_0 \frac{1}{M} \sum_{l=0}^{2M-1} |\, T_c[m,l]\,|^2 = P_d\, g_0 \tag{40}$$

and from (33), (28) and (38) it follows that

$$E\left[\left|\hat{D}_m[i]\right|^2\right] = P_d \left(|\, g_0\,|^2 \sum_{k=0}^{2M-1} \sum_{q} \left| \frac{1}{M} \sum_{l=0}^{2M-1} T_c[k, l+(i-q)M]\, T_c^*[m,l] \right|^2 + \frac{1}{SNR} \right)$$

$$= P_d \left(2\ |\, g_0\,|^2 + \frac{1}{SNR} \right). \tag{41}$$

Since in this case $E\left[\hat{D}_m^2[i]\right] = 0$, the optimum single-tap value (22) reduces to

$$a_m^{\text{flat}} = \frac{2\, E^*\left[d_m[i]\hat{D}_m[i]\right]}{E\left[|\, \hat{D}_m[i]\,|^2\right]} = \frac{g_0^*}{|\, g_0\,|^2 + \frac{1}{2\, SNR}} \tag{42}$$

and, moreover, since

$$\rho = \frac{\displaystyle\sum_{k=0}^{2M-1} \sum_{q} w_{m,k}^2 (i-q)}{\displaystyle\sum_{k=0}^{2M-1} \sum_{q} \left| w_{m,k}(i-q) \right|^2 + \frac{1}{SNR}} = 0 \tag{43}$$

and

$$u = \frac{P_d\, w_{m,m}^2(0)}{\displaystyle\sum_{k=0}^{2M-1} \sum_{q} \left| w_{m,k}(i-q) \right|^2 + \frac{1}{SNR}} = \frac{P_d\, g_0^2}{2\,|\, g_0\,|^2 + \frac{1}{SNR}} \tag{44}$$

the minimum MSE value results to be

$$E\left[\epsilon^2\right]_{\min}^{\text{flat}} = P_d \left(1 - \frac{|\, g_0\,|^2}{|\, g_0\,|^2 + \frac{1}{2\, SNR}} \right). \tag{45}$$

5. The asymptotic case ($M \gg 1$)

Let us now suppose that M is sufficiently large with respect to the maximum excess delay of the channel [14]. In this case, the prototype filter has contained time-variations, so that, for each value of θ_p and $l \in \{0, 1, \ldots, 2M-1\}$ it follows that

$$T_c[k, l-\theta_p] = h[l-\theta_p]\, e^{j\frac{\pi}{M}\left(k+\frac{1}{2}\right)\left(l-\theta_p+\frac{1}{2}+\frac{M}{2}\right)} \simeq h[l]\, e^{j\frac{\pi}{M}\left(k+\frac{1}{2}\right)\left(l-\theta_p+\frac{1}{2}+\frac{M}{2}\right)} = T_c[k, l] e^{-j\frac{\pi}{M}\left(k+\frac{1}{2}\right)\theta_p}. \tag{46}$$

By substituting (46) in (28), we obtain

$$\begin{aligned} w_{m,k}(i-q) &= \frac{1}{M} \sum_{p=0}^{L-1} g_p \sum_{l=0}^{2M-1} T_c[k, l-\theta_p + (i-q)M]\, T_c^*[m, l] \\ &\simeq \frac{1}{M} \sum_{p=0}^{L-1} g_p e^{-j\frac{\pi}{M}\left(k+\frac{1}{2}\right)\theta_p} \sum_{l=0}^{2M-1} T_c[k, l + (i-q)M]\, T_c^*[m, l] \\ &= H_c\left(\frac{2k+1}{4M}\right) \frac{1}{M} \sum_{l=0}^{2M-1} T_c[k, l + (i-q)M]\, T_c^*[m, l] \end{aligned} \tag{47}$$

where $H_c\left(\frac{2k+1}{4M}\right)$ is the frequency response of the multipath channel at frequency $F = \frac{2k+1}{4M}$. Therefore, we can write

$$\begin{aligned} E\left[\hat{D}_m^2[i]\right] &= P_d \sum_{k=0}^{2M-1} \sum_{q} w_{m,k}^2(i-q) \\ &\simeq P_d \sum_{k=0}^{2M-1} H_c^2\left(\frac{2k+1}{4M}\right) \sum_{q} \left(\frac{1}{M} \sum_{l=0}^{2M-1} T_c[k, l + (i-q)M] T_c^*[m, l] \right)^2 \\ &= P_d \sum_{k=0}^{2M-1} H_c^2\left(\frac{2k+1}{4M}\right) \left(\frac{1}{M} \sum_{l=0}^{2M-1} T_c[k, l+M] T_c^*[m, l] \right)^2 \\ &\quad + P_d \sum_{k=0}^{2M-1} H_c^2\left(\frac{2k+1}{4M}\right) \left(\frac{1}{M} \sum_{l=0}^{2M-1} T_c[k, l] T_c^*[m, l] \right)^2 \\ &\quad + P_d \sum_{k=0}^{2M-1} H_c^2\left(\frac{2k+1}{4M}\right) \left(\frac{1}{M} \sum_{l=0}^{2M-1} T_c[k, l-M] T_c^*[m, l] \right)^2. \end{aligned} \tag{48}$$

In particular, the last equality holds since for the considered prototype filter (see (13)) the only three values of q to be considered are $q \in \{i-1, i, i+1\}$. Moreover, in Appendix E, taking into account (6) and the considered prototype filter (13), it is shown that

$$\frac{1}{M} \sum_{l=0}^{2M-1} T_c[k, l+M]\, T_c^*[m, l] = (-1)^m\, j\, \xi(k-m)\,, \tag{49}$$

$$\frac{1}{M} \sum_{l=0}^{2M-1} T_c[k, l]\, T_c^*[m, l] = \delta[k-m] + \frac{j}{2}\, \delta[k-m+1] - \frac{j}{2}\, \delta[k-m-1]\,, \tag{50}$$

and

$$\frac{1}{M} \sum_{l=0}^{2M-1} T_c[k, l-M]\, T_c^*[m, l] = (-1)^{k+1}\, j\, \xi(k-m) \tag{51}$$

where

$$\xi(l) \triangleq \frac{1}{4M} \left\{ \frac{\sin\left[\frac{\pi}{2}(l+1)\right]}{\sin\left[\frac{\pi}{2M}(l+1)\right]} + \frac{\sin\left[\frac{\pi}{2}(l-1)\right]}{\sin\left[\frac{\pi}{2M}(l-1)\right]} \right\}. \tag{52}$$

Let us observe that $\xi^2(l)$ is periodic with period $2M$ and, moreover, as shown in Appendix F, it results

$$\sum_{l=0}^{2M-1} \xi^2(l) = \frac{1}{4}\,. \tag{53}$$

By substituting (49), (50) and (51) in (48) it follows that

$$E\left[\hat{D}_m^2[i]\right] \simeq P_d \left[H_c^2\left(\frac{2m+1}{4M}\right) - \frac{1}{4}\, H_c^2\left(\frac{2m-1}{4M}\right) - \frac{1}{4}\, H_c^2\left(\frac{2m+3}{4M}\right) \right]$$

$$-2\, P_d \sum_{k=0}^{2M-1} H_c^2\left(\frac{2k+1}{4M}\right) \xi^2(k-m)\,. \tag{54}$$

Let us observe that, from (53) and (54) it follows that if the value of M is sufficiently large that the channel frequency response $H_c(F)$ is flat in a range of subcarriers such that $\xi^2(\pm l)$ becomes negligible we obtain

$$E\left[\hat{D}_m^2[i]\right] \simeq 0\,. \tag{55}$$

Moreover, taking into account (46) we can write

$$E\left[d_m[i]\hat{D}_m[i]\right] = P_d\, w_{m,m}(0) = P_d\,\frac{1}{M}\sum_{p=0}^{L-1} g_p \sum_{l=0}^{2M-1} T_c[m, l-\theta_p]\, T_c^*[m,l]$$

$$\simeq P_d\, H_c\left(\frac{2m+1}{4M}\right)\frac{1}{M}\sum_{l=0}^{2M-1}|T_c[m,l]|^2 = P_d\, H_c\left(\frac{2m+1}{4M}\right) \tag{56}$$

and

$$E\left[\left|\hat{D}_m[i]\right|^2\right] = P_d\left(\sum_{k=0}^{2M-1}\sum_{q}\left|w_{m,k}(i-q)\right|^2 + \frac{1}{SNR}\right)$$

$$\simeq P_d\left(\sum_{k=0}^{2M-1}\left|H_c\left(\frac{2k+1}{4M}\right)\right|^2\sum_{q}\left|\frac{1}{M}\sum_{l=0}^{2M-1} T_c[k, l+(i-q)M]\, T_c^*[m,l]\right|^2 + \frac{1}{SNR}\right). \tag{57}$$

By substituting (49), (50) and (51) in (57) it follows that

$$E\left[\left|\hat{D}_m[i]\right|^2\right] \simeq P_d\left[\left|H_c\left(\frac{2m+1}{4M}\right)\right|^2 + \frac{1}{4}\left|H_c\left(\frac{2m-1}{4M}\right)\right|^2 + \frac{1}{4}\left|H_c\left(\frac{2m+3}{4M}\right)\right|^2\right]$$

$$+2\,P_d\sum_{k=0}^{2M-1}\left|H_c\left(\frac{2k+1}{4M}\right)\right|^2\xi^2(k-m) + P_d\,\frac{1}{SNR}. \tag{58}$$

Let us observe that, from (53) and (58) it follows that if the value of M is sufficiently large that the channel frequency response $H_c(F)$ is flat in a range of subcarriers such that $\xi^2(\pm l)$ becomes negligible we obtain

$$E\left[\left|\hat{D}_m[i]\right|^2\right] \simeq P_d\left(2\left|H_c\left(\frac{2m+1}{4M}\right)\right|^2 + \frac{1}{SNR}\right). \tag{59}$$

Thus, if M is sufficiently large that (55) and (59) hold, taking into account (56) the optimum single-tap (22) results to be

$$a_m^{\text{asy}} = \frac{H_c^*\left(\frac{2m+1}{4M}\right)}{\left|H_c\left(\frac{2m+1}{4M}\right)\right|^2 + \frac{1}{2\,SNR}} \tag{60}$$

and, the corresponding minimum MSE results to be

$$E\left[\epsilon^2\right]_{\min}^{\text{asy}} = P_d\left(1 - \frac{\left|H_c\left(\frac{2m+1}{4M}\right)\right|^2}{\left|H_c\left(\frac{2m+1}{4M}\right)\right|^2 + \frac{1}{2\,SNR}}\right). \tag{61}$$

Thus, for high SNR values the optimum MMSE single-tap (for large values of M) a_m^{asy} in (60) is nearly equal to the gain adopted in the well-known zero-forcing single-tap receiver

$$a_m^{\text{zf}} = \frac{1}{H_c\left(\frac{2m+1}{4M}\right)} \tag{62}$$

based on the approximation of the gain in (30) for large values of M.

6. Simulation results

In this section the BER of the optimum MMSE single-tap receiver (labeled as SC MMSE) based on (22) in frequency-selective Rayleigh fading channel is assessed via computer simulations and compared with that of the single-tap equalizer (labeled as SC) based on (30), the exact expression of the gain of the useful term in the decision variable [15], that of the single-tap equalizer (labeled as SCA) based on (62) and that of the asymptotic ($M \gg 1$) expression of the optimum MMSE single-tap receiver (labeled as SCA MMSE) based on (22). In the figures the performance of the 2M-4M receiver equalizer is also reported, and, moreover, the BER in the ideal interference-free condition [15] is presented. The simulation results are obtained under the following conditions:

1. the transmitted data belong to a 2-PAM and a 8-PAM constellation and in the active subcarriers profile 1 (ASP1) the percentage of active subcarriers is 89%, moreover, in the active subcarriers profile 2 (ASP2), profile 1 is modified by inserting one virtual subcarrier between active subcarriers to simulate a scenario where a fragmented spectrum is considered;
2. the considered Extended Vehicular A (EVA) [16] multipath channel model has the following power/delay profile: relative power (in dB) equal to [0 − 1.5 − 1.4 − 3.6 − 0.6 − 9.1 − 7 − 12 − 16.9] and excess tap delay (in discrete samples) [0 1 3 6 7 14 22 35 50]. Moreover, the considered multipath channel model Extended Typical Urban (ETU) [16] has

the following power/delay profile: relative power (expressed in dB) equal to $[-1 \;\; -1 \;\; -1 \;\; 0 \;\; 0 \;\; 0 \;\; -3 \;\; -5 \;\; -7]$ and excess tap delay (expressed in discrete samples) equal to [0 1 2 4 5 10 32 46 100];

3. the BER values are obtained by averaging over all the active subcarriers of a given multicarrier symbol in a burst and over 10^4 independent channel realizations in the 2-PAM case and over 10^3 independent channel realizations in the 8-PAM case;
4. each channel realization is assumed to be perfectly known and remains constant in the whole burst.

Figures 1 and 2 show the BER of the considered receivers versus E_b/N_o for 2-PAM constellation and $M = 64$ in EVA channel, and for the active subcarriers profiles 1 and 2, respectively. The results show that, when ASP1 is considered the asymptotic versions of the single-tap structures, particularly that of the MMSE structure, perform worse than the other single-tap structures, and, moreover, the 2M-4M receiver provides the best performance. Note that taking into account (31), (32) and (33) the asymptotic version of the solution of (22) leads to an approximation of a many terms, this can lead to a performance degradation with respect to the other considered less complex single-tap structures. On the other side, when ASP2 is considered, the MMSE SC receiver outperforms the remaining single-tap receivers and, moreover, assures a performance slightly worse than that of the 2M-4M receiver. Thus, when ASP2 is considered the solution of (22) leads to a gain that can allow to exploit the noncircularity of the zero-mean output of the standard receiver based on the matched filter. Figures 3 and 4 show the BER of the considered receivers for $M = 128$ in EVA channel and for the active subcarriers profiles 1 and 2, respectively. When ASP1 is considered all the receivers present a performance improvement and, moreover, the performance gap between the 2M-4M receiver and the other single-tap receivers is reduced. In the

ASP2 case all the single-tap structures assure similar performance except for the MMSE single-tap receiver that, for high values of E_b/N_o slightly outperforms the other considered structures.

Figures 5 and 6 show the BER of the considered receivers for 2-PAM constellation and $M = 128$ in ETU channel, and for the active subcarriers profiles 1 and 2, respectively. Moreover, figures 7 (ASP1) and 8 (ASP1) show the BER for $M = 256$. The results show that, in the ASP1 case the 2M-4M receiver outperforms all the single-tap structures, moreover, for $M = 128$ a performance degradation of the structures designed for large values of M (SCA and SCA MMSE) is observed while for $M = 256$ only the degradation of the SCA MMSE structure is present. In the ASP2 case when $M = 128$ the MMSE single-tap structure clearly outperforms the other single-tap structures and presents a contained performance degradation with respect to the 2M-4M receiver. Furthermore, when $M = 256$ the MMSE single-tap receiver assures a performance practically coincident with that of the 2M-4M structure and both outperform for high values of E_b/N_o the other considered single-tap receivers.

Figures 9 and 10 show the BER of the considered receivers versus E_b/N_o for 8-PAM constellation and $M = 64$ in EVA channel, and for the active subcarriers profiles 1 and 2, respectively. The results show that when ASP1 is considered the 2M-4M receiver clearly outperforms the other considered structures while when ASP2 is considered a performance improvement of the SC MMSE receiver with respect to the other considered single-tap structures can be observed. However, this improvement is not observed for larger values of M. Moreover, figures 11 (ASP1) and 12 (ASP2) show that for $M = 256$ only the 2M-4M receiver assures a contained performance degradation with respect to the interference-free curve in the whole range of values of E_b/N_o.

Finally, figures 13 and 14 show the BER of the considered receivers for 8-PAM

constellation and $M = 128$ in ETU channel, and for the active subcarriers profiles 1 and 2, respectively. Moreover, figures 15 (ASP1) and 16 (ASP1) show the BER for $M = 512$. The results show that only in the ASP2 case when $M = 128$ the MMSE single-tap structure outperforms the other single-tap structures. However, as M becomes larger this performance improvement disappears.

7. Conclusions

The FBMC-PAM transceiver with its capabilities in terms of spectral efficiency, asynchronous access and protection of adjacent users, has the potential to meet many requirements imposed by the future wireless systems [17].

In this paper the problem of single-tap equalization of FBMC-PAM signals in wireless dispersive channels has been analyzed. The MMSE single-tap receiver has been derived and its performance has been compared with that of other previously considered receivers. It has been shown that the MMSE single-tap gain assumes a more involved expression when the output of the standard matched filter (that multiplied by the considered gain, provides, after real part extraction, the decision variable) is noncircular. In this case the MMSE single-tap receiver can outperform other single-tap structures and can assure a performance similar to that of the more advanced 2M-4M equalizer. However, the observed performance improvement of the MMSE SC receiver with respect to the other considered single-tap structures is more contained as the constellation size increases.

Appendix A

In this appendix we provide some detail about the solution of (18) which is reported here for readability

$$a_m E\left[\hat{D}_m^2[i]\right] + a_m^* E\left[\left|\hat{D}_m[i]\right|^2\right] = 2E\left[d_m[i]\hat{D}_m[i]\right]. \tag{A.1}$$

By using the definitions

$$E\left[\hat{D}_m^2[i]\right] \triangleq \alpha^R + j\alpha^I$$

$$E\left[\left|\hat{D}_m[i]\right|^2\right] \triangleq \beta$$

$$E\left[d_m[i]\hat{D}_m[i]\right] \triangleq \zeta^R + j\zeta^I$$

(A.1) leads to the following system of two real equations

$$\begin{cases} a_m^R\left(\alpha^R + \beta\right) - a_m^I\,\alpha^I &= 2\zeta^R \\ \\ a_m^R\,\alpha^I + a_m^I\left(\alpha^R - \beta\right) &= 2\zeta^I. \end{cases} \tag{A.2}$$

where $a_m^R = \Re\{a_m\}$ and $a_m^I = \Im\{a_m\}$. The solution of this system is

$$a_m^R = \frac{2\,\Re\left\{E^*\left[\hat{D}_m^2[i]\right]E\left[d_m[i]\hat{D}_m[i]\right]\right\} - 2E\left[\left|\hat{D}_m[i]\right|^2\right]\Re\left\{E\left[d_m[i]\hat{D}_m[i]\right]\right\}}{\left|E\left[\hat{D}_m^2[i]\right]\right|^2 - E^2\left[\left|\hat{D}_m[i]\right|^2\right]} \tag{A.3}$$

$$a_m^I = \frac{2\,\Im\left\{E^*\left[\hat{D}_m^2[i]\right]E\left[d_m[i]\hat{D}_m[i]\right]\right\} + 2E\left[\left|\hat{D}_m[i]\right|^2\right]\Im\left\{E\left[d_m[i]\hat{D}_m[i]\right]\right\}}{\left|E\left[\hat{D}_m^2[i]\right]\right|^2 - E^2\left[\left|\hat{D}_m[i]\right|^2\right]} \tag{A.4}$$

Therefore, we can write

$$a_m = a_m^R + ja_m^I = \frac{2\,E^*\left[\hat{D}_m^2[i]\right]E\left[d_m[i]\hat{D}_m[i]\right] - 2E\left[\left|\hat{D}_m[i]\right|^2\right]E^*\left[d_m[i]\hat{D}_m[i]\right]}{\left|E\left[\hat{D}_m^2[i]\right]\right|^2 - E^2\left[\left|\hat{D}_m[i]\right|^2\right]}. \tag{A.5}$$

Appendix B

In this appendix we provide some detail about the steps that lead to the expression of the minimum MSE value in (23) obtained by substituting (22) in (17) reported here for readability

$$E\left[\epsilon^2\right] = \frac{1}{2}\Re\left\{a_m^2 E\left[\hat{D}_m^2[i]\right]\right\} + \frac{1}{2} \mid a_m \mid^2 E\left[\left|\hat{D}_m[i]\right|^2\right] + P_d - 2\Re\left\{a_m E\left[d_m[i]\hat{D}_m[i]\right]\right\} . \tag{B.1}$$

By using the definitions

$$E\left[\hat{D}_m^2[i]\right] \triangleq \alpha \tag{B.2}$$

$$E\left[\left|\hat{D}_m[i]\right|^2\right] \triangleq \beta \tag{B.3}$$

$$E\left[d_m[i]\hat{D}_m[i]\right] \triangleq \zeta \tag{B.4}$$

we can write

$$E\left[\epsilon^2\right] = \frac{1}{2}\Re\left\{a_m^2\alpha\right\} + \frac{1}{2} \mid a_m \mid^2 \beta + P_d - 2\Re\left\{a_m\zeta\right\} . \tag{B.5}$$

Since the optimum complex gain results to be (see (A.5))

$$a_m = \frac{2\alpha^*\zeta - 2\beta\zeta^*}{|\alpha|^2 - \beta^2} = \frac{2\alpha^*\zeta - 2\beta\zeta^*}{\delta} \tag{B.6}$$

where

$$\delta \triangleq |\alpha|^2 - \beta^2 \tag{B.7}$$

the minimum value of the MSE results to be

$$E\left[\epsilon^2\right]_{\min} = \frac{2}{\delta^2}\Re\left\{(\alpha^*\zeta - \beta\zeta^*)^2\,\alpha\right\} + \frac{2}{\delta^2}|\alpha^*\zeta - \beta\zeta^*|^2\beta + P_d - \frac{4}{\delta}\Re\left\{(\alpha^*\zeta - \beta\zeta^*)\,\zeta\right\}$$

$$= \frac{2}{\delta^2}\Re\left\{\alpha^*\zeta^2\right\}\left[\mid\alpha\mid^2 - \beta^2\right] - \frac{2}{\delta^2}\beta \mid \zeta \mid^2 \left[\mid\alpha\mid^2 - \beta^2\right] + P_d - \frac{4}{\delta}\Re\left\{\alpha^*\zeta^2\right\} + \frac{4}{\delta}\beta \mid \zeta \mid^2 .$$

Taking into account the definition of δ in (B.7) we can write

$$E\left[\epsilon^2\right]_{\min} = \frac{2}{\delta^2}\Re\left\{\alpha^*\zeta^2\right\}\delta - \frac{2}{\delta^2}\beta \mid \zeta \mid^2 \delta + P_d - \frac{4}{\delta}\Re\left\{\alpha^*\zeta^2\right\} + \frac{4}{\delta}\beta \mid \zeta \mid^2$$

$$= P_d - \frac{2}{\delta}\Re\left\{\alpha^*\zeta^2\right\} + \frac{2}{\delta}\beta \mid \zeta \mid^2 .$$

Finally, by using the definitions (B.2), (B.3), (B.4), and (B.7), the expression of the minimum MSE value in (23) immediately follows.

Appendix C

In this appendix we derive the relationship (37). Let us observe that, since $T_c[2M+k, l+qM] = -T_c[k, l+qM]$ (see (6)), we can equivalently show that

$$\sum_{k=0}^{2M-1} \sum_{q} \left(\frac{1}{M} \sum_{l=0}^{2M-1} T_c[m+k, l+qM]\, T_c^*[m, l] \right)^2 = 0\,. \tag{C.1}$$

Taking into account (6) we can write

$$\sum_{k=0}^{2M-1} \sum_{q} \left(\frac{1}{M} \sum_{l=0}^{2M-1} T_c[m+k, l+qM]\, T_c^*[m, l] \right)^2$$

$$= \frac{1}{M^2} \sum_{k=0}^{2M-1} \sum_{q} \left(e^{j\frac{\pi}{M}\left(m+k+\frac{1}{2}\right)qM} \right)^2 \left(\sum_{l=0}^{2M-1} h[l+qM]\, e^{j\frac{\pi}{M}\left(m+k+\frac{1}{2}\right)\left(l+\frac{1}{2}+\frac{M}{2}\right)}\, h[l]\, e^{-j\frac{\pi}{M}\left(m+\frac{1}{2}\right)\left(l+\frac{1}{2}+\frac{M}{2}\right)} \right)^2$$

$$= \frac{1}{M^2} \sum_{q} e^{j\pi q} \sum_{l_1=0}^{2M-1} \sum_{l_2=0}^{2M-1} h[l_1+qM]\, h[l_2+qM]\; h[l_1]\, h[l_2] \sum_{k=0}^{2M-1} e^{j\frac{\pi}{M}k(l_1+l_2+1+M)}\,. \tag{C.2}$$

Let us observe that

$$\sum_{k=0}^{2M-1} e^{j\frac{\pi}{M}k(l_1+l_2+1+M)} = \begin{cases} 2M & \text{if } \; l_1+l_2+1+M = 2M\,r \\ \\ 0 & \text{otherwise}\,. \end{cases} \tag{C.3}$$

Since $l_1, l_2 \in \{0, 1, \ldots, 2M-1\}$ the sum in (C.3) is different from zero only for $l_2 = M-1-l_1$ with $l_1 \in \{0, 1, \ldots, M-1\}$, and for $l_2 = 3M-1-l_1$ with $l_1 \in \{M, M+1, \ldots, 2M-1\}$, thus we can write

$$\sum_{k=0}^{2M-1} \sum_{q} \left(\frac{1}{M} \sum_{l=0}^{2M-1} T_c[m+k, l+qM]\, T_c^*[m, l] \right)^2$$

$$= \frac{1}{M^2} \sum_{q} e^{j\pi q} \left\{ \sum_{l_1=0}^{M-1} h[l_1+qM]\, h[l_1]\, h[M-1-l_1]\, h[M-1-l_1+qM] \right.$$

$$\left. + \sum_{l_1=M}^{2M-1} h[l_1+qM]\, h[l_1]\, h[3M-l_1-1]\, h[3M-l_1-1+qM] \right\}. \tag{C.4}$$

Taking into account the symmetry condition (9) it follows that

$$h[M-1-l_1] = h[M+l_1] \tag{C.5}$$

$$h[M-1-l_1+qM] = h[M-1-(l_1-qM)] = h[M+l_1-qM] \tag{C.6}$$

$$h[3M-1-l_1] = h[M+\underbrace{2M-1-l_1}_{u}] = h[M-1-u] = h[l_1-M] \tag{C.7}$$

$$h[3M-1-l_1+qM] = h[M+\underbrace{2M-1-l_1+qM}_{u}] = h[M-1-u] = h[l_1-M-qM] \tag{C.8}$$

By substituting (C.5) - (C.8) in (C.4) we obtain

$$\sum_{k=0}^{2M-1}\sum_{q}\left(\frac{1}{M}\sum_{l=0}^{2M-1} T_c[m+k,l+qM]\,T_c^*[m,l]\right)^2$$

$$= \frac{1}{M^2}\sum_{q} e^{j\pi q}\left\{\sum_{l_1=0}^{M-1} h[l_1+qM]\,h[l_1]\,h[l_1+M]\,h[l_1+M-qM] + \sum_{l_1=M}^{2M-1} h[l_1+qM]\,h[l_1]\,h[l_1-M]\,h[l_1-M-qM]\right\} \tag{C.9}$$

By using the position $l = l_1 - M$ in the last sum in (C.9) we obtain

$$\sum_{k=0}^{2M-1}\sum_{q}\left(\frac{1}{M}\sum_{l=0}^{2M-1} T_c[m+k,l+qM]\,T_c^*[m,l]\right)^2$$

$$= \frac{1}{M^2}\sum_{q} e^{j\pi q}\left\{\sum_{l_1=0}^{M-1} h[l_1+qM]\,h[l_1]\,h[l_1+M]\,h[l_1+M-qM] + \sum_{l=0}^{M-1} h[l+M+qM]\,h[l+M]\,h[l]\,h[l-qM]\right\} \tag{C.10}$$

and, then, we can write

$$\sum_{k=0}^{2M-1}\sum_{q}\left(\frac{1}{M}\sum_{l=0}^{2M-1} T_c[m+k,l+qM]\,T_c^*[m,l]\right)^2$$

$$= \frac{1}{M^2}\left\{\sum_{l_1=0}^{M-1} h[l_1]\,h[l_1]\,h[l_1+M]\,h[l_1+M] + \sum_{l=0}^{M-1} h[l+M]\,h[l+M]\,h[l]\,h[l]\right.$$

$$
\begin{aligned}
&- \sum_{l_1=0}^{M-1} h[l_1 - M]\, h[l_1]\, h[l_1 + M]\, h[l_1 + 2M] \; - \sum_{l=0}^{M-1} h[l]\, h[l + M]\, h[l]\, h[l + M] \\
&- \sum_{l_1=0}^{M-1} h[l_1 + M]\, h[l_1]\, h[l_1 + M]\, h[l_1] \; - \sum_{l=0}^{M-1} h[l + 2M]\, h[l + M]\, h[l]\, h[l - M] \Bigg\} \\
&= \frac{1}{M^2} \left\{ 2 \sum_{l=0}^{M-1} h^2[l]\, h^2[l + M] \; - \sum_{l=0}^{M-1} h^2[l]\, h^2[l + M] \; - \sum_{l_1=0}^{M-1} h^2[l_1]\, h^2[l_1 + M] \right\} = 0
\end{aligned}
\tag{C.11}
$$

Appendix D

In this appendix we show the relationship (38). A similar result has been shown in the Appendix of [18] with reference to the FBMC-OQAM signal case.

Let us observe that, since $T_c[2M + k, l + qM] = -T_c[k, l + qM]$ (see (6)), we can equivalently show that

$$
\sum_{k=0}^{2M-1} \sum_{q} \left| \frac{1}{M} \sum_{l=0}^{2M-1} T_c[m + k, l + qM]\, T_c^*[m, l] \right|^2 = 2\,. \tag{D.1}
$$

Taking into account (6) we can write

$$
\begin{aligned}
&\sum_{k=0}^{2M-1} \sum_{q} \left| \frac{1}{M} \sum_{l=0}^{2M-1} T_c[m + k, l + qM]\, T_c^*[m, l] \right|^2 \\
&= \frac{1}{M^2} \sum_{q} \sum_{l_1=0}^{2M-1} \sum_{l_2=0}^{2M-1} h[l_1 + qM]\, h[l_2 + qM]\; h[l_1]\, h[l_2] \sum_{k=0}^{2M-1} e^{j\frac{\pi}{M}k(l_1 - l_2)}\,.
\end{aligned}
\tag{D.2}
$$

Let us observe that

$$
\sum_{k=0}^{2M-1} e^{j\frac{\pi}{M}k(l_1 - l_2)} = \begin{cases} 2M & \text{if } \; l_1 - l_2 = 2M\, r \\ \\ 0 & \text{otherwise}\,. \end{cases} \tag{D.3}
$$

Since $l_1, l_2 \in \{0, 1, \ldots, 2M - 1\}$ the sum in (D.3) is different from zero only for $l_2 = l_1$ with $l_1 \in \{0, 1, \ldots, 2M - 1\}$, thus we can write

$$
\sum_{k=0}^{2M-1} \sum_{q} \left| \frac{1}{M} \sum_{l=0}^{2M-1} T_c[m + k, l + qM]\, T_c^*[m, l] \right|^2 = \frac{2}{M} \sum_{q} \sum_{l_1=0}^{2M-1} h^2[l_1 + qM]\, h^2[l_1]\,. \tag{D.4}
$$

Taking into account condition (10) for $r = 0$ it follows that

$$\frac{2}{M}\sum_{l_1=0}^{2M-1} h^2[l_1] \underbrace{\sum_{q} h^2[l_1 + qM]}_{=1} = \frac{2}{M}\sum_{l_1=0}^{2M-1} h^2[l_1] = 2\,. \tag{D.5}$$

Finally, from (D.5) and (D.4) equation (38) follows.

Appendix E

In this appendix, with reference to the adopted prototype filter in (13), we evaluate the explicit expression of the terms

$$t(k, m, i-q) \triangleq \frac{1}{M}\sum_{l=0}^{2M-1} T_c[k, l + (i-q)M]\, T_c^*[m, l] \tag{E.1}$$

in (48). Let us observe that since the length of the prototype filter in (13) is $L_h = 2M$, it immediately follows that $t(k, m, i-q) \neq 0$ only for $i - q = -1, 0, 1$.

Let us evaluate $t(k, m, 0)$, taking into account (6) we obtain

$$t(k, m, i) \triangleq \frac{1}{M}\sum_{l=0}^{2M-1} T_c[k, l]\, T_c^*[m, l] = \frac{1}{M}\sum_{l=0}^{2M-1} h^2[l] e^{j\frac{\pi}{M}(k-m)\left(l+\frac{1}{2}+\frac{M}{2}\right)}\,. \tag{E.2}$$

Since, for $l = 0, 1, \ldots, 2M-1$,

$$h^2[l] = \frac{1}{2} - \frac{1}{2}\cos\left[\frac{\pi}{M}\left(l + \frac{1}{2}\right)\right]$$

it follows that

$$\frac{1}{M}\sum_{l=0}^{2M-1} h^2[l] e^{j\frac{\pi}{M}(k-m)\left(l+\frac{1}{2}+\frac{M}{2}\right)} = \frac{1}{M}\sum_{l=0}^{2M-1}\left\{\frac{1}{2} - \frac{1}{2}\cos\left[\frac{\pi}{M}\left(l + \frac{1}{2}\right)\right]\right\} e^{j\frac{\pi}{M}(k-m)\left(l+\frac{1}{2}+\frac{M}{2}\right)}$$

$$= \frac{1}{2M} e^{j\frac{\pi}{M}(k-m)\left(\frac{1}{2}+\frac{M}{2}\right)}\left\{\sum_{l=0}^{2M-1} e^{j\frac{\pi}{M}(k-m)\,l} - \frac{1}{2}e^{j\frac{\pi}{2M}}\sum_{l=0}^{2M-1} e^{j\frac{\pi}{M}(k-m+1)\,l} - \frac{1}{2}e^{-j\frac{\pi}{2M}}\sum_{l=0}^{2M-1} e^{j\frac{\pi}{M}(k-m-1)\,l}\right\}$$

$$= e^{j\frac{\pi}{M}(k-m)\left(\frac{1}{2}+\frac{M}{2}\right)}\left\{\delta[k-m] - \frac{1}{2}e^{j\frac{\pi}{2M}}\delta[k-m+1] - \frac{1}{2}e^{-j\frac{\pi}{2M}}\delta[k-m-1]\right\}$$

$$= \delta[k-m] - \frac{1}{2}\,e^{-j\frac{\pi}{2}}\,\delta[k-m+1] - \frac{1}{2}\,e^{j\frac{\pi}{2}}\,\delta[k-m-1]\,.$$

Therefore, we can write

$$t(k,m,0) \triangleq \frac{1}{M}\sum_{l=0}^{2M-1} T_c[k,l]\,T_c^*[m,l] = \delta[k-m]+\frac{j}{2}\,\delta[k-m+1]-\frac{j}{2}\,\delta[k-m-1] \quad \text{(E.3)}$$

Let us now evaluate $t(k,m,1)$, taking into account (6) we obtain

$$t(k,m,1) \triangleq \frac{1}{M}\sum_{l=0}^{2M-1} T_c[k,l+M]\,T_c^*[m,l] = e^{j\frac{\pi}{M}\left(k+\frac{1}{2}\right)M}\frac{1}{M}\sum_{l=0}^{2M-1} h[l+M]\,h[l]\,e^{j\frac{\pi}{M}(k-m)\left(l+\frac{1}{2}+\frac{M}{2}\right)}$$

$$= e^{j\frac{\pi}{M}\left(k+\frac{1}{2}\right)M}A = (-1)^k\,jA$$

where

$$A \triangleq \frac{1}{M}\sum_{l=0}^{M-1} h[l+M]\,h[l]\,e^{j\frac{\pi}{M}(k-m)\left(l+\frac{1}{2}+\frac{M}{2}\right)} \quad \text{(E.4)}$$

$$= \frac{1}{M}\sum_{l=0}^{M-1}\sin\left[\frac{\pi}{2M}\left(l+M+\frac{1}{2}\right)\right]\sin\left[\frac{\pi}{2M}\left(l+\frac{1}{2}\right)\right]e^{j\frac{\pi}{M}(k-m)\left(l+\frac{1}{2}+\frac{M}{2}\right)}$$

$$= \frac{1}{4jM}e^{j\frac{\pi}{M}(k-m)\left(\frac{1}{2}+\frac{M}{2}\right)}\left\{e^{j\frac{\pi}{2M}}\sum_{l=0}^{M-1}e^{j\frac{\pi}{M}(k-m+1)\,l} - e^{-j\frac{\pi}{2M}}\sum_{l=0}^{M-1}e^{j\frac{\pi}{M}(k-m-1)\,l}\right\}$$

$$= \frac{1}{4M}(-1)^{(k-m)}\left\{\frac{\sin\left[\frac{\pi}{2}(k-m+1)\right]}{\sin\left[\frac{\pi}{2M}(k-m+1)\right]}+\frac{\sin\left[\frac{\pi}{2}(k-m-1)\right]}{\sin\left[\frac{\pi}{2M}(k-m-1)\right]}\right\}$$

Therefore,

$$t(m,k,1) \triangleq \frac{1}{M}\sum_{l=0}^{2M-1} T_c[k,l+M]\,T_c^*[m,l]$$

$$= (-1)^m\,j\,\frac{1}{4M}\left\{\frac{\sin\left[\frac{\pi}{2}(k-m+1)\right]}{\sin\left[\frac{\pi}{2M}(k-m+1)\right]}+\frac{\sin\left[\frac{\pi}{2}(k-m-1)\right]}{\sin\left[\frac{\pi}{2M}(k-m-1)\right]}\right\}. \quad \text{(E.5)}$$

Let us now evaluate $t(k,m,-1)$, taking into account (6) we obtain

$$t(k,m,-1) \triangleq \frac{1}{M}\sum_{l=0}^{2M-1} T_c[k,l-M]\,T_c^*[m,l] = e^{-j\frac{\pi}{M}\left(k+\frac{1}{2}\right)M}\frac{1}{M}\sum_{l=0}^{2M-1} h[l-M]\,h[l]\,e^{j\frac{\pi}{M}(k-m)\left(l+\frac{1}{2}+\frac{M}{2}\right)}$$

$$= e^{-j\frac{\pi}{M}\left(k+\frac{1}{2}\right)M}B = (-1)^k\,(-j)\,B$$

where

$$B \triangleq \frac{1}{M}\sum_{l=0}^{2M-1} h[l-M]\,h[l]\,e^{j\frac{\pi}{M}(k-m)\left(l+\frac{1}{2}+\frac{M}{2}\right)} = \frac{1}{M}\sum_{l=M}^{2M-1} h[l-M]\,h[l]\,e^{j\frac{\pi}{M}(k-m)\left(l+\frac{1}{2}+\frac{M}{2}\right)}.$$

By using the position $l_1 = l - M$ we obtain

$$B = \frac{1}{M} \sum_{l_1=0}^{M-1} h[l_1]h[l_1 + M]e^{j\frac{\pi}{M}(k-m)\left(l_1+M+\frac{1}{2}+\frac{M}{2}\right)}$$

$$= e^{j\frac{\pi}{M}(k-m)\,M} \frac{1}{M} \sum_{l_1=0}^{M-1} h[l_1]h[l_1 + M]e^{j\frac{\pi}{M}(k-m)\left(l_1+\frac{1}{2}+\frac{M}{2}\right)} = e^{j\frac{\pi}{M}(k-m)\,M} A = (-1)^{(k-m)} A\,.$$

Therefore, we can write

$$t(k, m, -1) = (-1)^k (-j)\, B$$

where

$$B = (-1)^{(k-m)} A$$

and, then, taking into account (E.4) we obtain

$$t(k, m, -1) \triangleq \frac{1}{M} \sum_{l=0}^{2M-1} T_c[k, l-M]\, T_c^*[m, l] = (-1)^k (-j)\, (-1)^{(k-m)} A = (-j)\, (-1)^m A$$

$$= (-j)\, (-1)^k \frac{1}{4M} \left\{ \frac{\sin\left[\frac{\pi}{2}\,(k-m+1)\right]}{\sin\left[\frac{\pi}{2M}\,(k-m+1)\right]} + \frac{\sin\left[\frac{\pi}{2}\,(k-m-1)\right]}{\sin\left[\frac{\pi}{2M}\,(k-m-1)\right]} \right\}. \qquad \text{(E.6)}$$

Appendix F

We have shown in Appendix C that

$$\sum_{k=0}^{2M-1} \sum_{q} \left| \frac{1}{M} \sum_{l=0}^{2M-1} T_c[m+k, l+qM]\, T_c^*[m, l] \right|^2 = 2\,. \qquad \text{(F.1)}$$

Since $q \in \{-1, 0, 1\}$ (see (6)), it follows that

$$\underbrace{\sum_{k=0}^{2M-1} \left| \frac{1}{M} \sum_{l=0}^{2M-1} T_c[m+k, l-M]\, T_c^*[m, l] \right|^2}_{A_1}$$

$$+ \underbrace{\sum_{k=0}^{2M-1} \left| \frac{1}{M} \sum_{l=0}^{2M-1} T_c[m+k, l]\, T_c^*[m, l] \right|^2}_{A_2}$$

$$+\underbrace{\sum_{k=0}^{2M-1}\left|\frac{1}{M}\sum_{l=0}^{2M-1}T_c[m+k,l+M]\,T_c^*[m,l]\right|^2}_{A_3}=2\,. \tag{F.2}$$

Moreover, taking into account (E.6) we can write

$$\frac{1}{M}\sum_{l=0}^{2M-1}T_c[m+k,l-M]\,T_c^*[m,l]=\,(-1)^{k+m+1}\,j\,\xi(k)\,, \tag{F.3}$$

from (E.3) it follows that

$$\frac{1}{M}\sum_{l=0}^{2M-1}T_c[m+k,l]\,T_c^*[m,l]=\delta[k]+\frac{j}{2}\delta[k+1]-\frac{j}{2}\delta[k-1]\,, \tag{F.4}$$

and, finally, taking into account (E.5) it follows that

$$\frac{1}{M}\sum_{l=0}^{2M-1}T_c[m+k,l+M]\,T_c^*[m,l]=\,(-1)^m\,j\,\xi(k) \tag{F.5}$$

where (the expression of $\xi(\cdot)$ is reported here for readability)

$$\xi(l)=\frac{1}{4M}\left\{\frac{\sin\left[\frac{\pi}{2}\,(l+1)\right]}{\sin\left[\frac{\pi}{2M}\,(l+1)\right]}+\frac{\sin\left[\frac{\pi}{2}\,(l-1)\right]}{\sin\left[\frac{\pi}{2M}\,(l-1)\right]}\right\}. \tag{F.6}$$

Thus, from (F.2), (F.3), (F.4) and (F.5) we obtain

$$A_1\triangleq\sum_{k=0}^{2M-1}\left|\frac{1}{M}\sum_{l=0}^{2M-1}T_c[m+k,l-M]\,T_c^*[m,l]\right|^2=\sum_{k=0}^{2M-1}\xi^2(k) \tag{F.7}$$

$$A_3\triangleq\sum_{k=0}^{2M-1}\left|\frac{1}{M}\sum_{l=0}^{2M-1}T_c[m+k,l+M]\,T_c^*[m,l]\right|^2=\sum_{k=0}^{2M-1}\xi^2(k) \tag{F.8}$$

$$A_2\triangleq\sum_{k=0}^{2M-1}\left|\frac{1}{M}\sum_{l=0}^{2M-1}T_c[m+k,l]\,T_c^*[m,l]\right|^2=\frac{3}{2} \tag{F.9}$$

and, then, from (F.2) it follows that

$$2\sum_{k=0}^{2M-1}\xi^2(k)+\frac{3}{2}=2\,. \tag{F.10}$$

Therefore, we can write

$$\sum_{k=0}^{2M-1}\xi^2(k)\;=\;\frac{1}{4}\,. \tag{F.11}$$

References

[1] Y. Medjahdi, S. Traverso, R. Gerzaguet, H. Shaïek. R. Zayani, D. Demmer, R. Zakatia, J.P. Doré, M. Ben Mabrouk, D.Le Ruyet, Y.Louët and D. Roviras, On the road to 5G: comparative study of physical layer in MTC context, IEEE Access. vol. 5, pp. 26556-26581, 2017.

[2] D. Pinchon, P. Siohan, Derivation of analytical expressions for flexible PR low complexity FBMC systems, Proc. of 21th European Signal Processing Conference (EUSIPCO 2013), pp. 1-5, Sept. 2013.

[3] J. Nadal, C.A. Nour, A. Baghdadi, Design and evaluation of a novel short prototype filter for OFDM/OQAM modulation, IEEE Access. vol. 6, pp. 19610-19625, March 2018.

[4] D. Mattera, M. Tanda, M. Bellanger, Filter bank multicarrier with PAM modulation for future wireless systems, Signal Processing 120 (2016), pp. 594-606.

[5] P. Sabeti, A. Farhang, N. Marchetti and L. Doyle, Performance Analysis of FBMC-PAM in Massive MIMO, 2016 IEEE Globecom Workshops (GC Wkshps), Washington, DC, USA, 2016, pp. 1-7.

[6] C. Sexton, Q. Bodinier, A. Farhang, N. Marchetti, F. Bader, Enabling asynchronous machine-type D2D communication using multiple waveforms in 5G, IEEE Internet of things journal, vol. 5, pp. 1307-1322, April 2018.

[7] R.W. Chang, Synthesis of band-limited orthogonal signals for multichannel data transmission, The Bell System Technical Journal 45 (10) (1966) 1775-1796.

[8] D. Mattera, M. Tanda, M. Bellanger, CFO sensitivity and efficient estimation

for the short filter multicarrier system FBMC-PAM, Signal Processing 164 (2019), pp. 10-19.

[9] F. Neeser, J. Massey, "Proper complex random processes with applications to information theory," IEEE Trans. Inf. Theory, vol. 39, pp. 1293–1302, July 1993.

[10] B. Picinbono, "On circularity," IEEE Trans. Signal Process., vol. 42, pp. 3473–3482, Dec. 1994.

[11] P.J. Schreier, "Bounds on the degree of impropriety of complex random vectors," IEEE Signal Processing Letters, vol. 15, pp. 190–193, 2008.

[12] J.P. Delmas, H. Abeida, "On the degree of second-order non-circularity of complex random variables," Proc. of 2008 IEEE International Conference on Acoustics, Speech, and. Signal Processing (ICASSP), March 30 - April 4, 2008, Las Vegas, Nevada, USA.

[13] D. H. Brandwood, "A complex gradient operator and its application in adaptive array theory," Proc. Inst. Elect. Eng., F, vol. 130, pp. 11–16, Feb. 1983.

[14] C. Lélé, J.P. Javaudin, R. Legouable, A. Skrzypczak, P. Siohan, Channel estimation methods for preamble-based OFDM/OQAM modulations, European Transactions on Telecommunications vol. 19, pp. 741-750, 2008.

[15] D. Mattera, M. Tanda, M. Bellanger, On the performance of FBMC-PAM systems in frequency-selective Rayleigh fading channels, Physical Communication 45 (2021) 101264.

[16] 3GPP TS 136 104 version 8.8.0 Release 8, 2010.

[17] M. Matthaiou, O. Yurduseven, H.Q. Ngo, D. Morales-Jimenez, S.L. Cotton, V.F. Fusco, The road to 6G: ten physical layer challenges for communications

engineers, IEEE Communications Magazine vol.59, no. 1, January 2021, pp. 64-69.

[18] C. Lélé, J.P. Javaudin, R. Legouable, A. Skrzypczak, P. Siohan, Channel estimation methods for preamble-based OFDM/OQAM modulations, Proc. of 13th European Wireless Conference, 1-4 April 2007, Paris, France.

List of figures

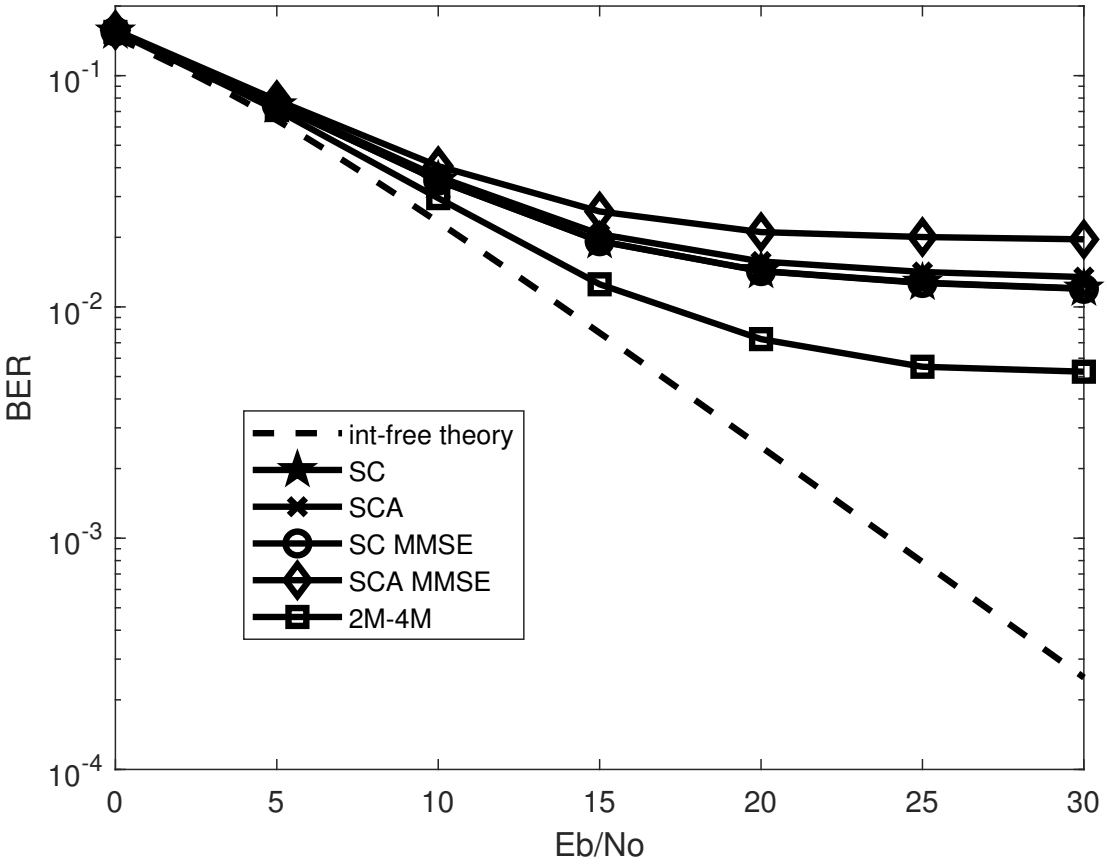

Figure 1: BER versus Eb/No over EVA channel for 2-PAM constellation, $M = 64$ and active subcarriers profile 1.

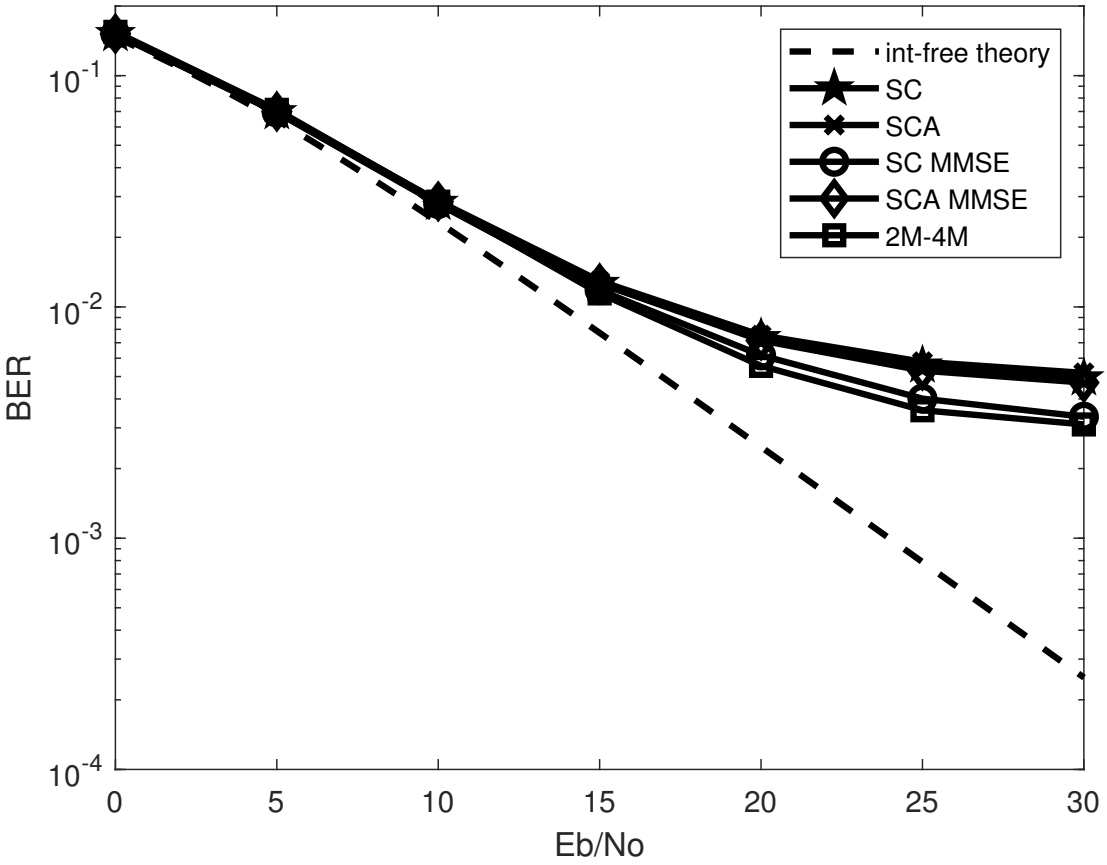

Figure 2: BER versus Eb/No over EVA channel for 2-PAM constellation, $M = 64$ and active subcarriers profile 2.

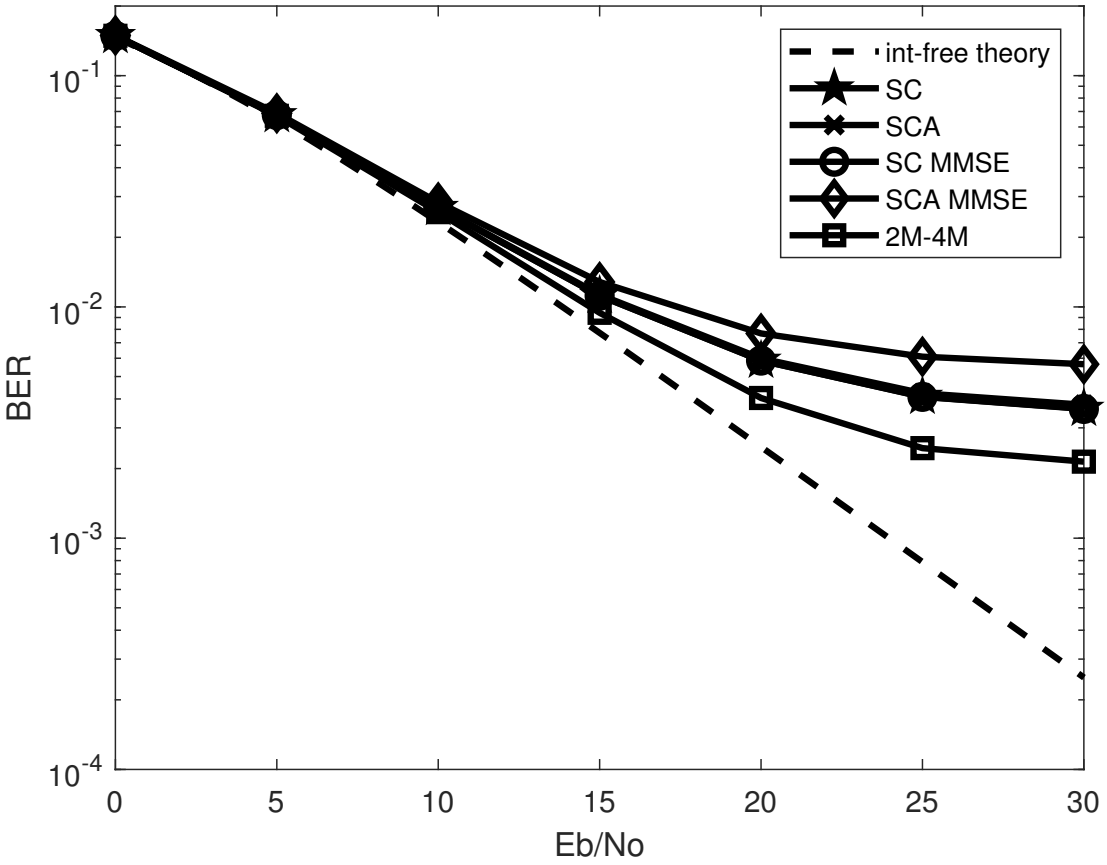

Figure 3: BER versus Eb/No over EVA channel for 2-PAM constellation, $M = 128$ and active subcarriers profile 1.

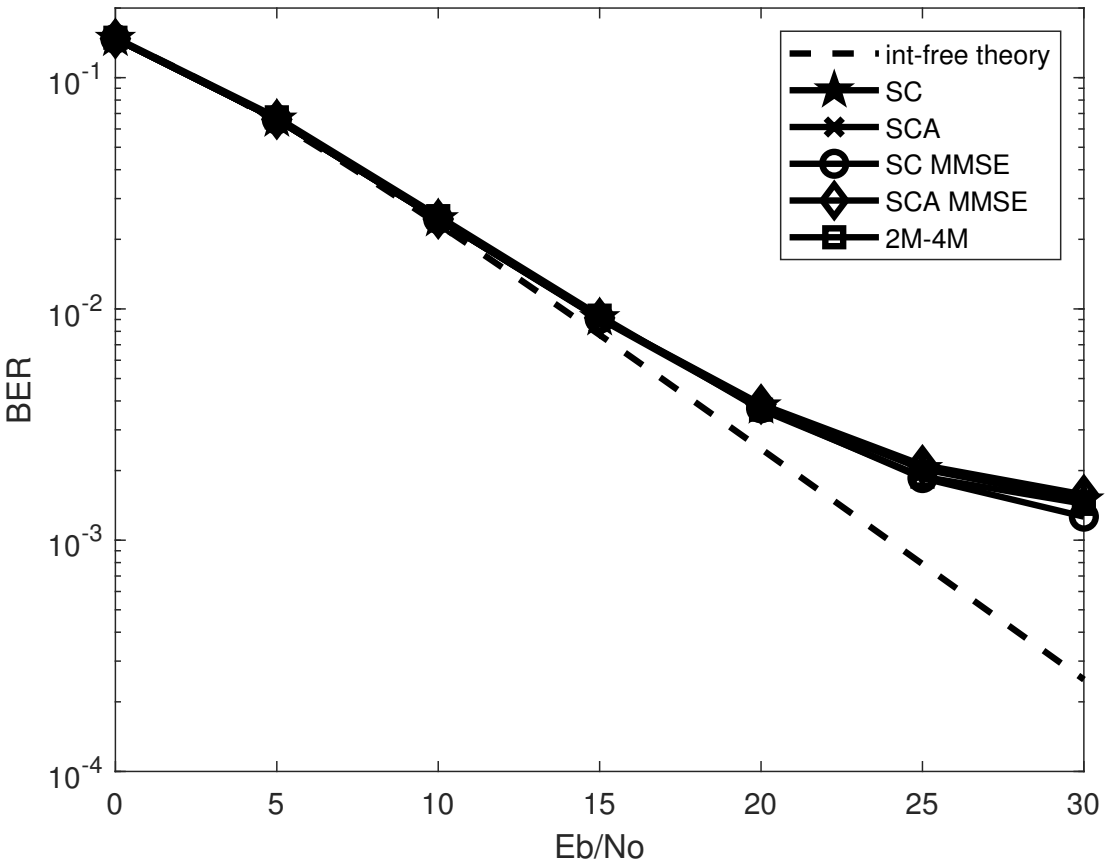

Figure 4: BER versus Eb/No over EVA channel for 2-PAM constellation, $M = 128$ and active subcarriers profile 2.

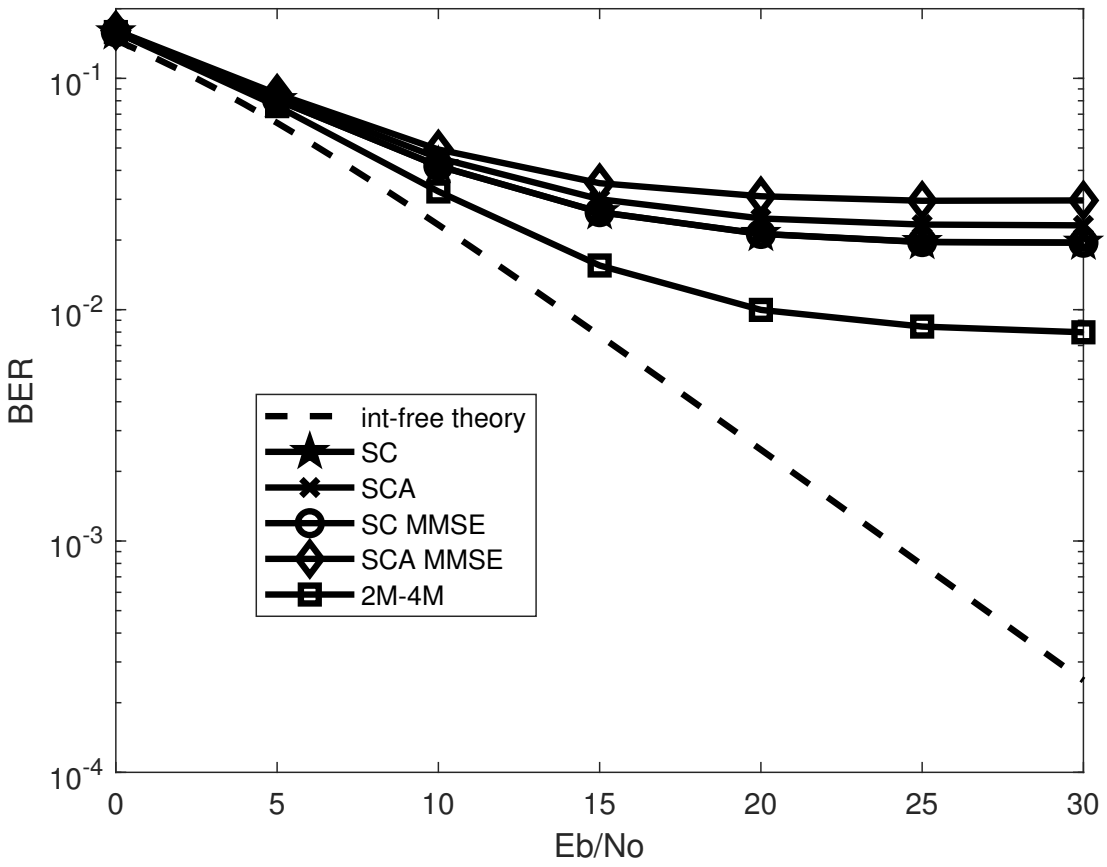

Figure 5: BER versus Eb/No over ETU channel for 2-PAM constellation, $M = 128$ and active subcarriers profile 1.

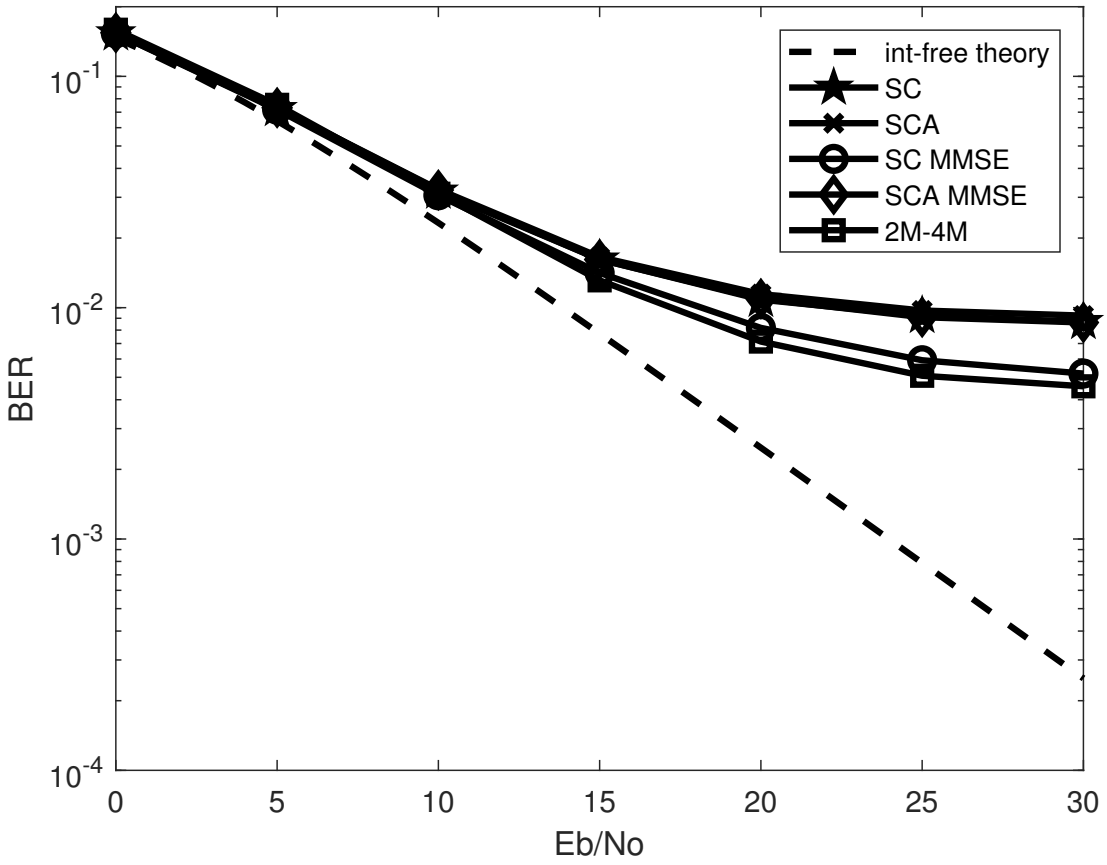

Figure 6: BER versus Eb/No over ETU channel for 2-PAM constellation, $M = 128$ and active subcarriers profile 2.

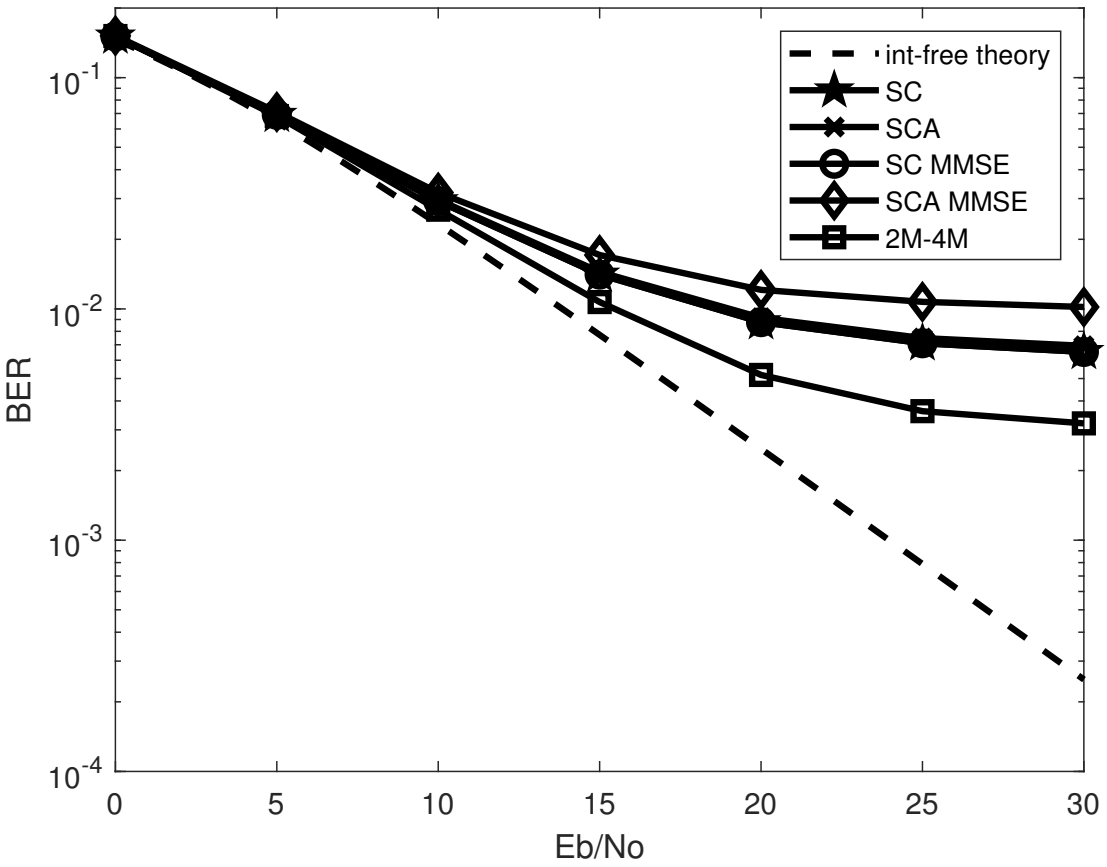

Figure 7: BER versus Eb/No over ETU channel for 2-PAM constellation, $M = 256$ and active subcarriers profile 1.

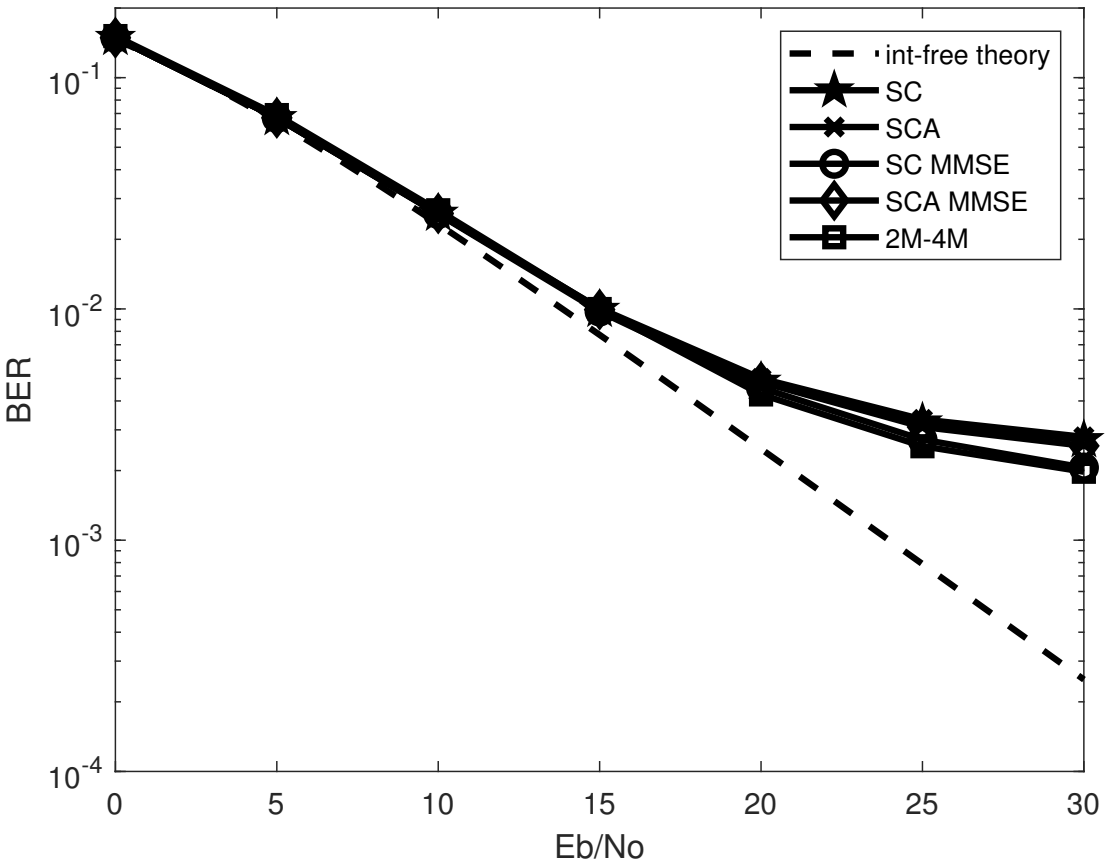

Figure 8: BER versus Eb/No over ETU channel for 2-PAM constellation, $M = 256$ and active subcarriers profile 2.

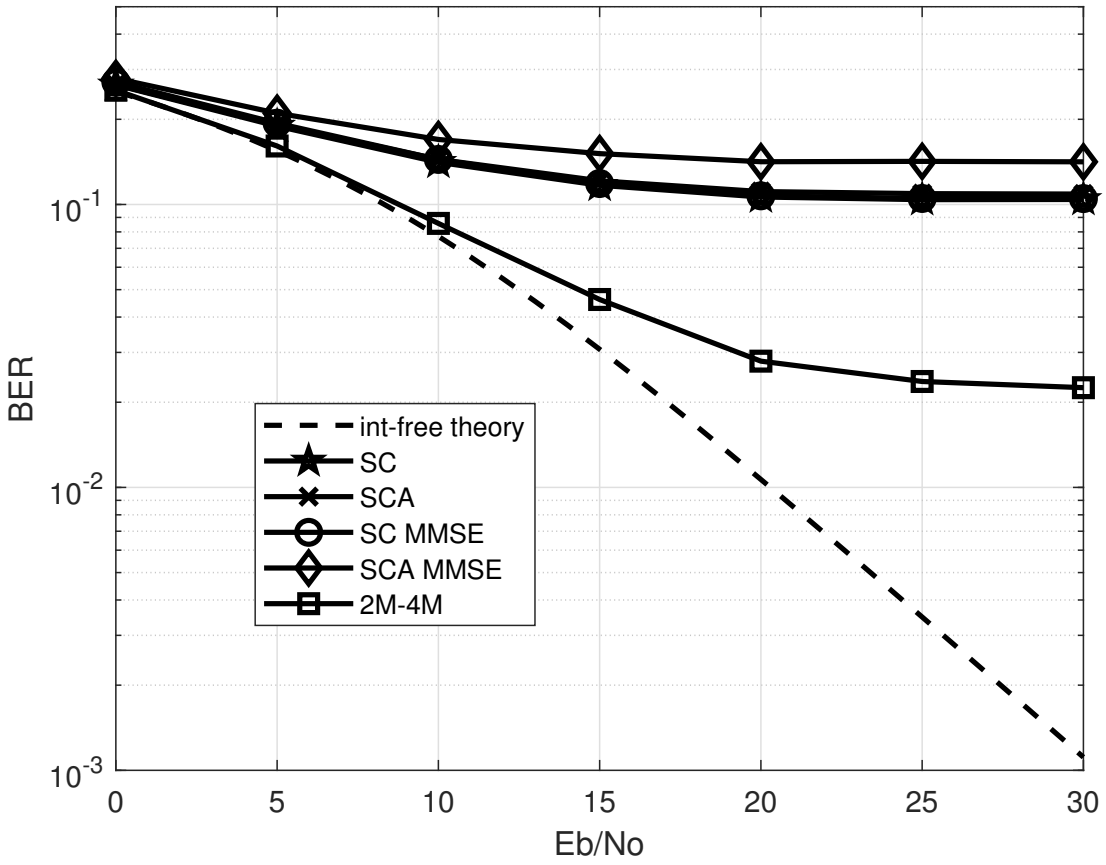

Figure 9: BER versus Eb/No over EVA channel for 8-PAM constellation, $M = 64$ and active subcarriers profile 1.

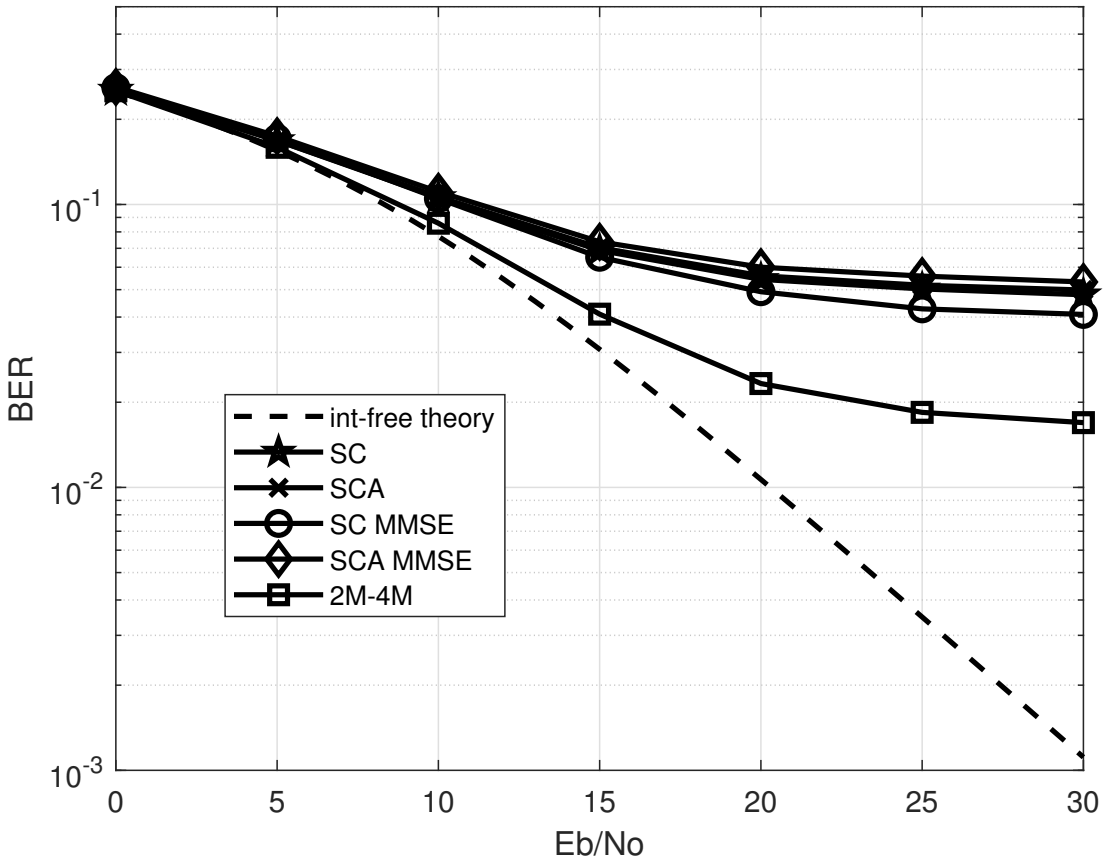

Figure 10: BER versus Eb/No over EVA channel for 8-PAM constellation, $M = 64$ and active subcarriers profile 2.

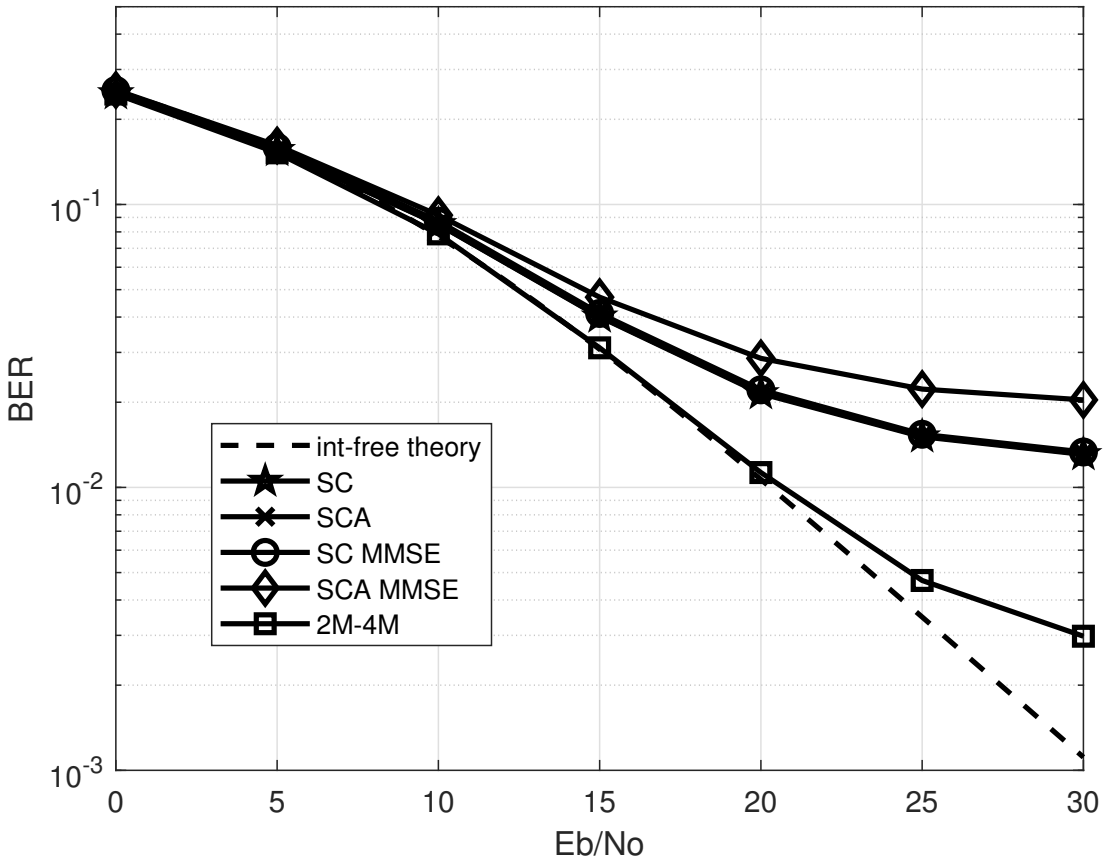

Figure 11: BER versus Eb/No over EVA channel for 8-PAM constellation, $M = 256$ and active subcarriers profile 1.

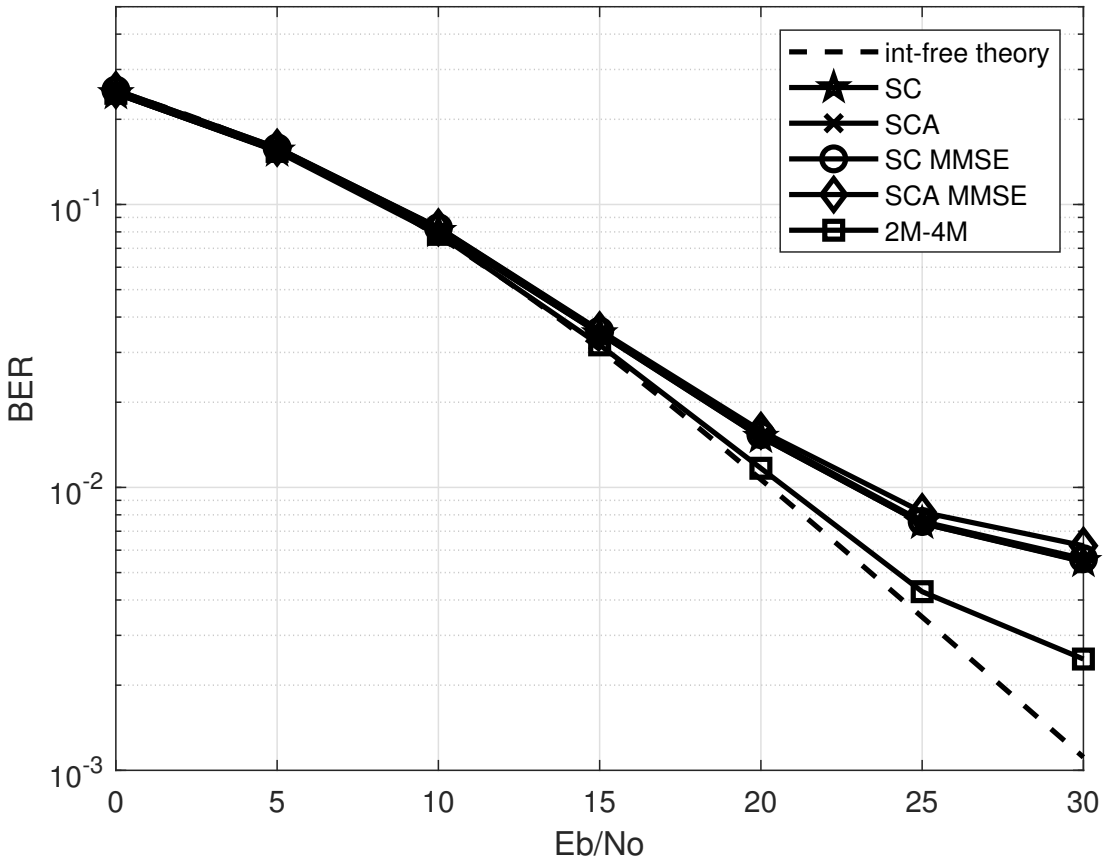

Figure 12: BER versus Eb/No over EVA channel for 8-PAM constellation, $M = 256$ and active subcarriers profile 2.

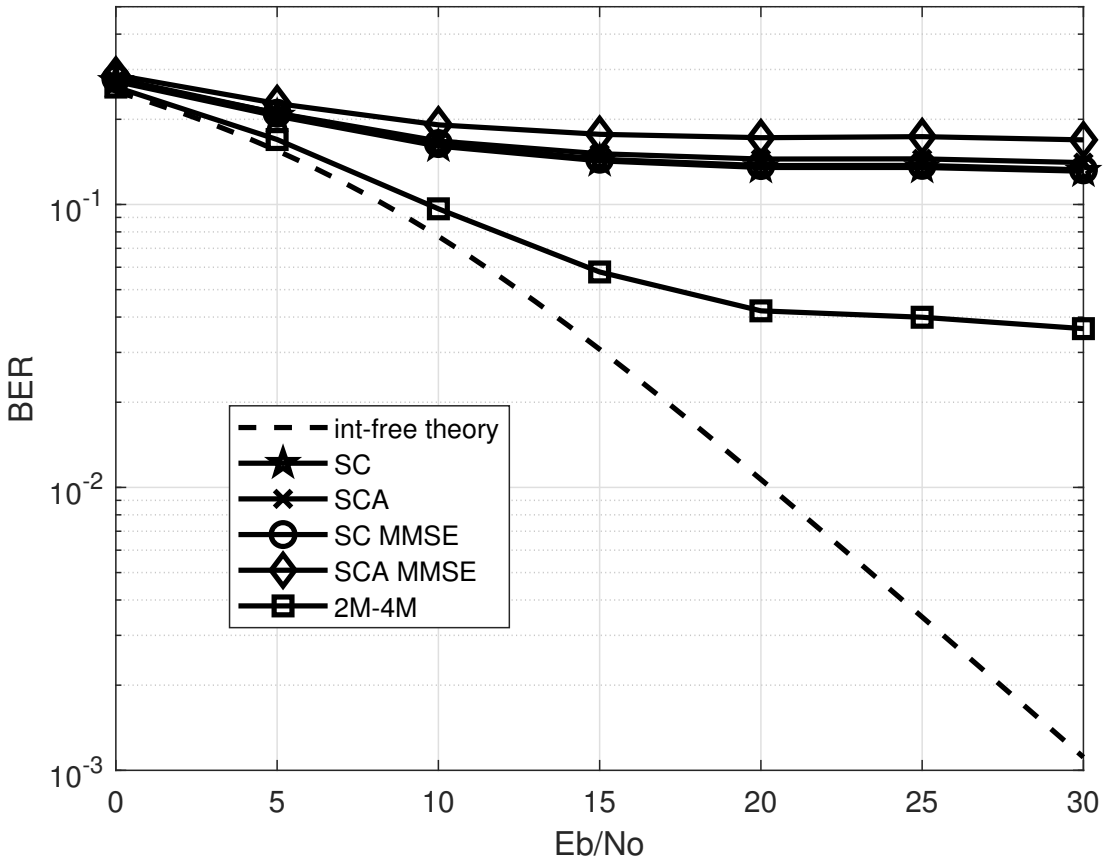

Figure 13: BER versus Eb/No over ETU channel for 8-PAM constellation, $M = 128$ and active subcarriers profile 1.

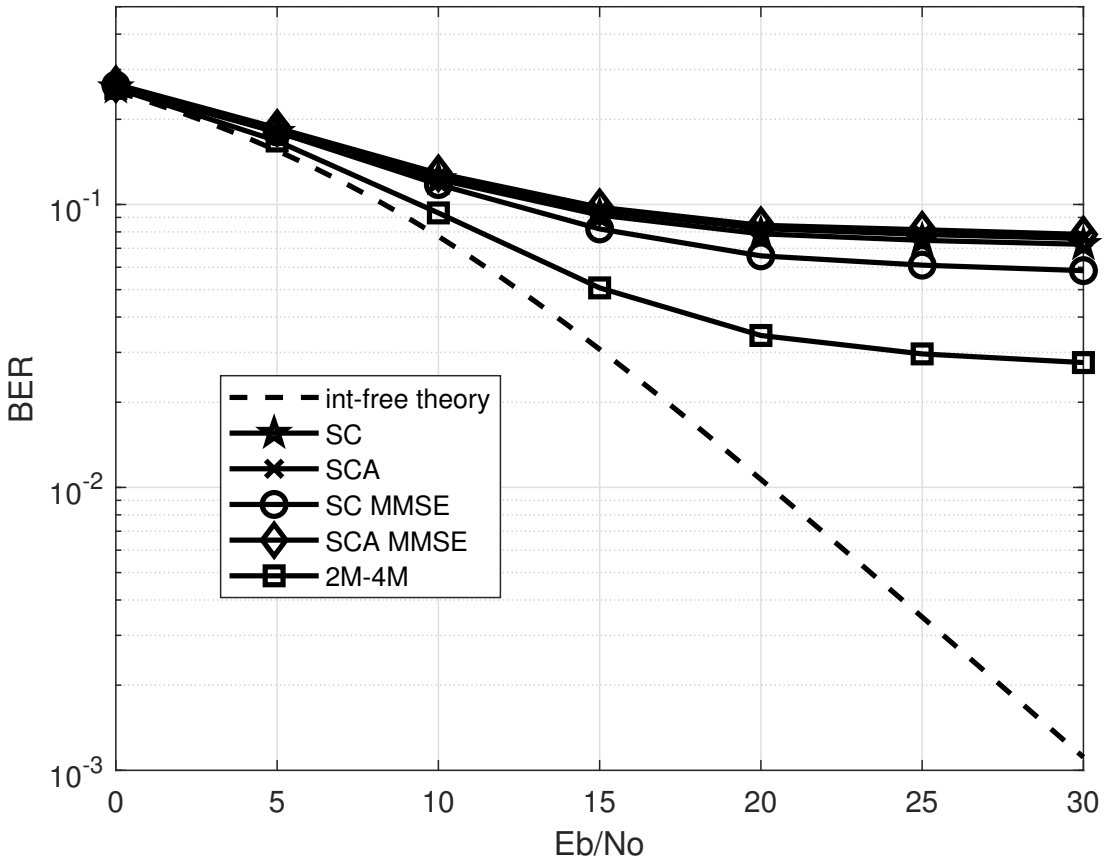

Figure 14: BER versus Eb/No over ETU channel for 8-PAM constellation, $M = 128$ and active subcarriers profile 2.

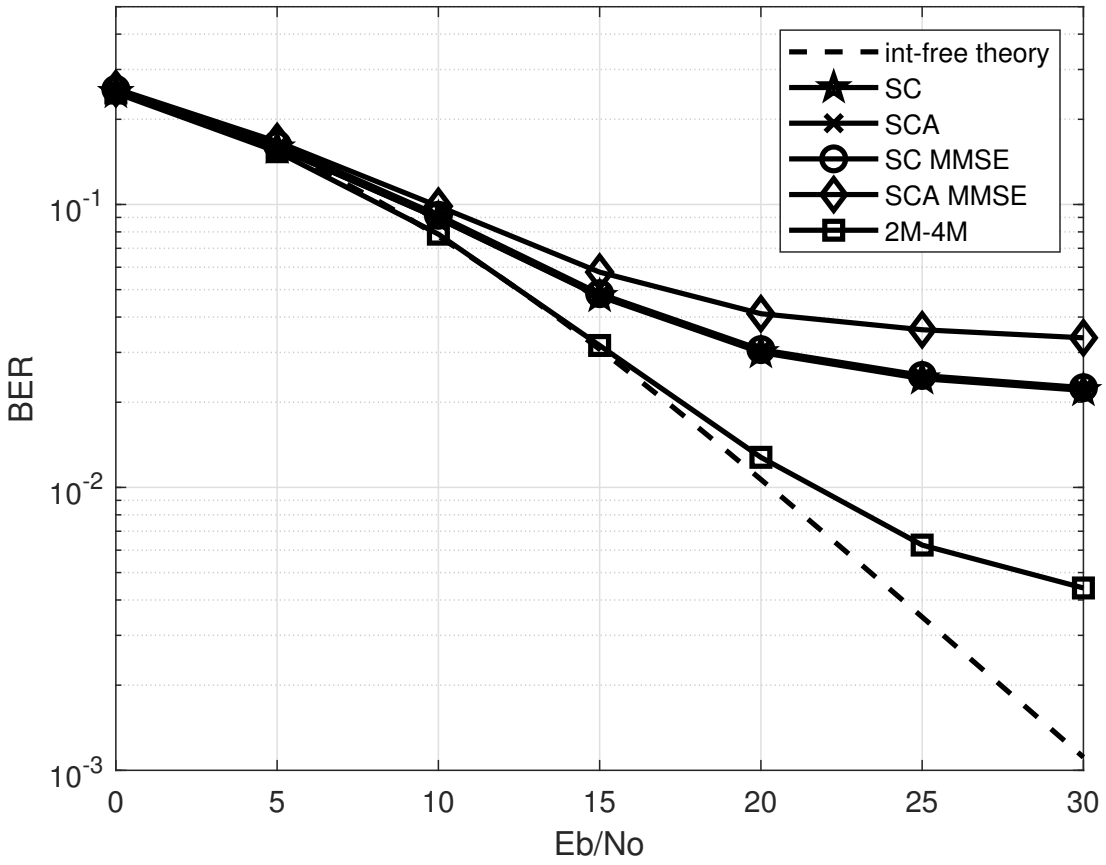

Figure 15: BER versus Eb/No over ETU channel for 8-PAM constellation, $M = 512$ and active subcarriers profile 1.

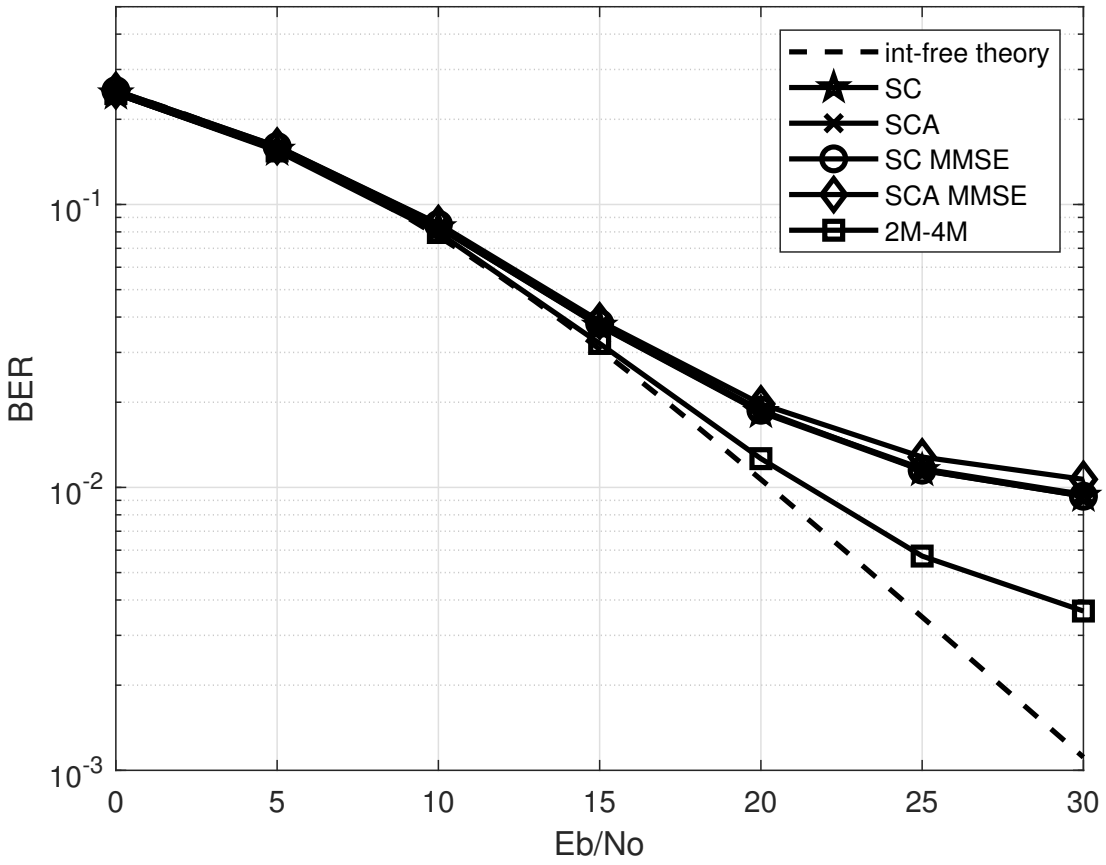

Figure 16: BER versus Eb/No over ETU channel for 8-PAM constellation, $M = 512$ and active subcarriers profile 2.